Nature and origin of collapse breccias in the Zechstein of NE England: local observations with cross-border petroleum exploration and production significance, across the North Sea

S. E. DANIELS[1]*, M. E. TUCKER[2], M. J. MAWSON[1], R. E. HOLDSWORTH[1,3], J. J. LONG[1], J. G. GLUYAS[3] & R. R. JONES[1]

[1]*Geospatial Research Ltd, Department of Earth Sciences, University of Durham, Durham DH1 3LE, UK*

[2]*School of Earth Sciences, University of Bristol, Wills Memorial Building, Queens Road, Bristol BS8 1RJ, UK*

[3]*Department of Earth Sciences, University of Durham, Durham DH1 3LE, UK*

SED, 0000-0001-9917-899X; MJM, 0000-0002-5517-9170; REH, 0000-0002-3467-835X; JGG, 0000-0002-9386-7206; RRJ, 0000-0003-4595-2489

Correspondence: susie@geospatial-research.com

Abstract: Hydrocarbon reservoirs hosted in Permian strata were some of the first to have been discovered in Europe. With discoveries in the Zechstein carbonates of Norway in recent years, and with exploration of Zechstein prospects both onshore and offshore UK, as well as in Dutch, Danish and Norwegian offshore sectors, understanding the architecture of the Zechstein carbonates remains very relevant. Here we study outcrops of Roker Formation carbonates (Z2, Ca2) in NE England to better understand geological processes associated with deformation following evaporite dissolution, with implications for exploration and production.

Collapse of Z2 Roker Formation strata in NE England, following the dissolution of *c.* 100 m or more of the Z1 Hartlepool Anhydrite, resulted in fundamental changes to the architecture of the succession. Complete dissolution of the anhydrite removed an effective regional seal and dramatically enhanced matrix and fracture permeability of the overlying Roker Formation. The collapsed Roker Formation can be vertically divided into three zones, based upon the degree of deformation. The lower zone and vertical collapse-breccia pipes that can extend across all zones have the highest permeabilities. The process of collapse was gradual, with local variations in the degree of brecciation. We derive a schematic sequence of collapse, recognizing the impact of mechanical barriers within the succession in retarding deformation up-section and it is this that ultimately leads to the vertical zonation.

Timing of evaporite dissolution is poorly constrained: it could have occurred soon after deposition, at the end of the Permian or during Tertiary uplift. It is known that evaporite dissolution has occurred offshore, with the oil fields Auk and Argyll (UK Central North Sea) given as examples of dissolution collapse-brecciated reservoirs. Reservoir quality is typically improved, with both matrix and fracture porosity and permeability enhanced. Complete evaporite dissolution could in some cases lead to the potential breach of the seal.

Dissolution collapse breccias are formed in the subsurface by the gravitational fragmentation and downward movement (or foundering) of sedimentary strata into voids created by the dissolution of underlying strata (Stanton 1966). Friedman (1997) highlighted the importance of evaporites, explaining that the rapid dissolution of sulfate (gypsum or anhydrite) can cause dissolution-collapse breccias to form in overlying carbonate strata. Collapse breccias can be regarded as a type of intrastratal karst (Ford & Williams 1989). Dissolution is typically attributed to the exposure of evaporite to meteoric water. Smith (1972) recognized that the degree of brecciation of carbonates overlying a dissolved evaporite linked to the quantity and distribution of sulfates that were originally associated with the carbonate, the original lithologies and competences, and the number and character of gravity-driven collapse events affecting the carbonates. Eliassen & Talbot (2005) described dissolution-collapse breccias around a Carboniferous basin in Central Spitzbergen. They noted different categories of breccia at different positions within the basin, with thick cross-cutting breccias up to 200 m thick in the central part of the basin (where

From: Patruno, S., Archer, S. G., Chiarella, D., Howell, J. A., Jackson, C. A.-L. & Kombrink, H. (eds) *Cross-Border Themes in Petroleum Geology I: The North Sea*. Geological Society, London, Special Publications, **494**, https://doi.org/10.1144/SP494-2019-140

evaporites were thickest), connected to horizontal strata-bound breccias interbedded with undeformed rocks in more marginal positions (where evaporites were thinner and interbedded with carbonates). They noted the presence of breccia pipes, alongside the observation that the effects of dissolution can resemble the effects of faulting, although without any large-scale lateral displacements, concluding that brecciation occurred in the subsurface, at moderate depths likely to be around 500 m (as constrained by the meteoric signature of cements and thickness of overlying units). Breccia pipes (also named dolines or sink-holes) can form at the surface or in the subsurface and represent focused sites of upward propagation of breakdown processes (stoping) in regions above dissolutional voids (Gutiérrez *et al.* 2008). The voids can be filled by sediments, making them 'buried sinkholes' (Gutiérrez *et al.* 2008). An additional effect of evaporite dissolution and contact with meteoric water can be dedolomitization (e.g. Smith 1972, 1995).

The Upper Permian Zechstein Group carbonate–evaporite deposits of NE England have been subject to burial and uplift, with associated diagenesis, faulting, fracturing, evaporite dissolution and collapse. The Zechstein succession of onshore England, as widely seen elsewhere in the Zechstein Basin, consists of three major carbonate–evaporite cycles (Z1, Z2, Z3), followed by thinner, more clastic–evaporite cycles in the upper part (Z4, Z5, Fig. 1). Of particular interest with the onshore outcrops in NE England is the occurrence of collapse breccias, spectacularly displayed along the coast of County Durham and Tyne and Wear. Foundering and brecciation within the Zechstein carbonates have been long recognized, since publications by Winch (1817) and Sedgwick (1829). Trechmann (1914) first linked this brecciation with evaporite dissolution, noting the absence of anhydrite at the surface compared with borehole data and the position of the brecciation above the anticipated level of anhydrite. Prior to this they were considered to be of tectonic origin (Woolacott

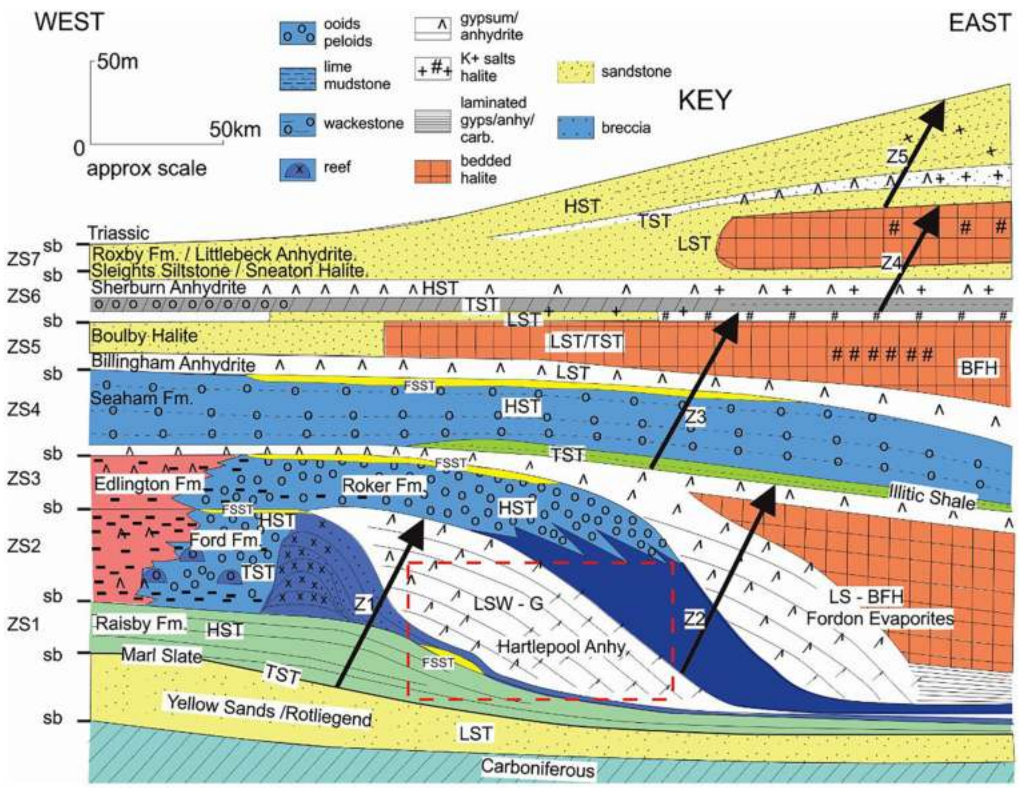

Fig. 1. Schematic cross-section for the Permian strata of NE England showing the formation names, broad lithofacies, carbonate evaporite cycles (black arrows, Z1 to Z5), and sequence stratigraphic scheme after Tucker (1991) (with recent modifications). Figure based on Tucker (1991), modified from Catuneanu *et al.* (2011). LST, lowstand systems tract; TST, transgressive systems tract; HST, highstand systems tract; FSST, falling stage systems tract; BFH, basin-fill halite; LSW-G, gypsum lowstand wedge; A./Anhy, anhydrite; H, halite; Slt, siltstone; Sh, shale; Sl, slate; Lst, limestone; Dol, dolomite; sb, sequence boundary. The red box indicates the stratigraphic interval discussed in this study.

1909). The most widespread unit affected by collapse brecciation is the Roker Formation (Z2 cycle carbonate) (Z2C or Ca2, equivalent to the Kirkham Abbey Formation of Yorkshire and Hauptdolomit of the North Sea and NW Europe), which is attributed to dissolution of the underlying Z1 anhydrite (i.e. the Hartlepool Anhydrite or Z1A, equivalent to the Werraanhydrit Formation). Cycle 3 (Z3) carbonates (the Seaham Formation, equivalent to the Plattendolomit Formation, Ca3) are also affected by dissolution of underlying evaporites (the Z2 Fordon Formation/Stassfurt evaporites, Smith 1994), visible at Seaham, although there are fewer exposures of these disturbed strata. In NE England, Smith (1972, 1994) suggested that evaporite dissolution occurred during Upper Cretaceous–Tertiary uplift, at a depth of at least 220 m, based on stratigraphic constraints derived from the thickness of overlying units involved in the process.

The Durham coast outcrops represent onshore analogues for Zechstein carbonate reservoirs within the Zechstein Basin of NW Europe (Figs 2 & 3) and should be useful for understanding similar carbonate–evaporite systems elsewhere in the world. Such reservoirs are well known in the Cambrian of the Tarim Basin, Ordovician of the Ordos Basin and Triassic of the Sichuan Basin in China (e.g. Jiang *et al.* 2018; Liu *et al.* 2019), and also the Carboniferous Madison Group of the USA (Sando 1967). The Paleozoic karst reservoir of the Loppa High, in the Norwegian Barents Sea, is also thought to be related to evaporite dissolution (Elvebakk *et al.* 2003; Eliassen & Talbot 2005).

The Zechstein carbonates were some of the first hydrocarbon reservoirs found in Europe; for example, there were Zechstein gas discoveries in Hamburg in 1910, and in the Eskdale Field, near Whitby, Yorkshire, UK, in 1938. UK North Sea oil production from Zechstein reservoirs began in the Argyll and Auk oilfields in 1975 and 1976 respectively, some production coming from collapse breccias (Robson 1991; Trewin & Bramwell 1991). Zechstein carbonate reservoirs are still significant (Fig. 2), as in Poland (for example the Barnówko-Mostno-Buszewo oil and gas field), Germany and The Netherlands (for example the onshore Schoonebeek, Drenthe Province and Friesland Province gas fields, P6 offshore gas field). In the UK both offshore (Auk and Argyll/Ardmore/Alma fields of the Central North Sea, Wissey and Hewett fields of the Southern North Sea (SNS)) and onshore (e.g. the Malton and Kirby Misperton fields of the Cleveland Basin) are hosted in Zechstein carbonates. There is current renewed exploration focus in the vicinity of the Mid North Sea High (MNSH) as a frontier area in a mature basin (Richardson *et al.* 2005; Patruno & Helland-Hansen 2018; Patruno *et al.* 2018, 2019). Oil is proven in the Zechstein

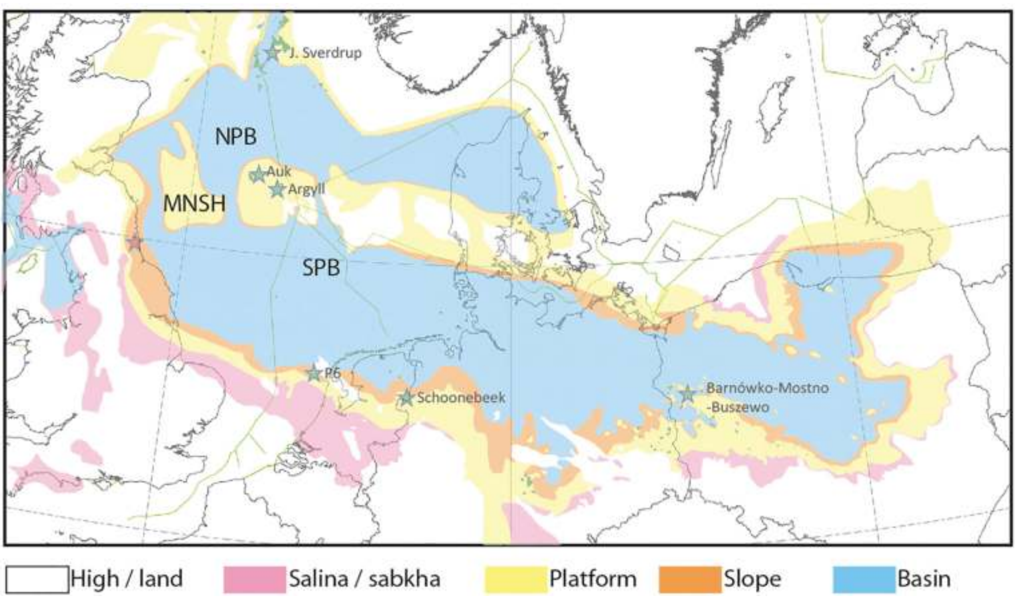

Fig. 2. Palaeogeography of the Z2 carbonate (Ca2) in the Permian Basin of NW Europe, after Słowakiewicz *et al.* (2015*a*). Red star locates the Zechstein outcrops in NE England where the study area is located, green stars locate hydrocarbon fields mentioned in the text. NPB, Northern Permian Basin; SPB, Southern Permian Basin; MNSH, Mid North Sea High.

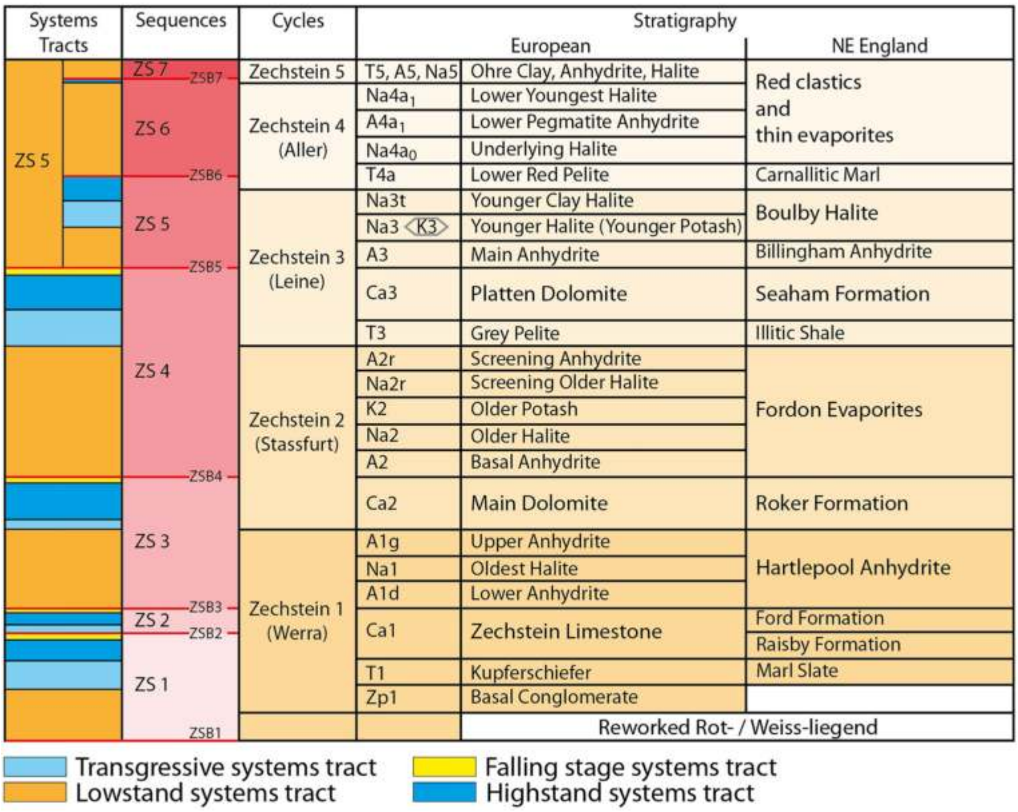

Fig. 3. The stratigraphic scheme for the Permian of NE England and the North Sea-continental Europe, with the abbreviations commonly used for the various units, plus the cycles and sequence stratigraphic interpretation (GRL 2016).

carbonates underlying the main Jurassic reservoir of the Johan Sverdrup Field, offshore Norway (Sorento *et al.* 2018). The second Zechstein cycle carbonates (Z2 in Fig. 1) are part of the most prolific reservoir in the Zechstein succession. Collapse brecciation related to evaporite dissolution has been recognized offshore around the margins of palaeohighs within the North Sea, such as the MNSH (e.g. in the Auk and Argyll fields, Trewin *et al.* 2003; Gluyas *et al.* 2005, respectively).

This article aims to: (1) describe the observed deformation associated with evaporite dissolution in spectacular exposures along the coast between Trow Point and Lizard Point, near Sunderland, in NE England (including famous examples in Marsden Bay, Figs 2 & 4); (2) make inferences about the process of collapse prompted by evaporite dissolution; (3) discuss timing constraints of this onshore collapse event; and (4) consider the implications for hydrocarbon exploration and production within similarly affected regions offshore.

Regional setting

The Zechstein Basin of NW Europe was a carbonate–evaporite basin during the Upper Permian, comprising two connected basins, the Southern and Northern Permian Basins (SPB, NPB), with a connection to an open ocean to the north, the Boreal–Panthalassa Sea, via a narrow seaway, 1000 km long (Doornenbal & Stevenson 2010), coincident with the later, Jurassic, Viking Graben. The sediments now exposed in NE England lay on the northwestern margin of the SPB (Fig. 2). The Permian succession, resting unconformably on Carboniferous strata, commences with the aeolian Yellow Sands, interpreted as seif draas (the onshore equivalent of part of the Rotliegend Formation) deposited across a vast, subsided desert basin, *c.* 200 m below sea-level (Doornenbal & Stevenson 2010). Marine inundation of this basin from the north led to the development of a cyclic carbonate–evaporite depositional system of the Zechstein Group. This

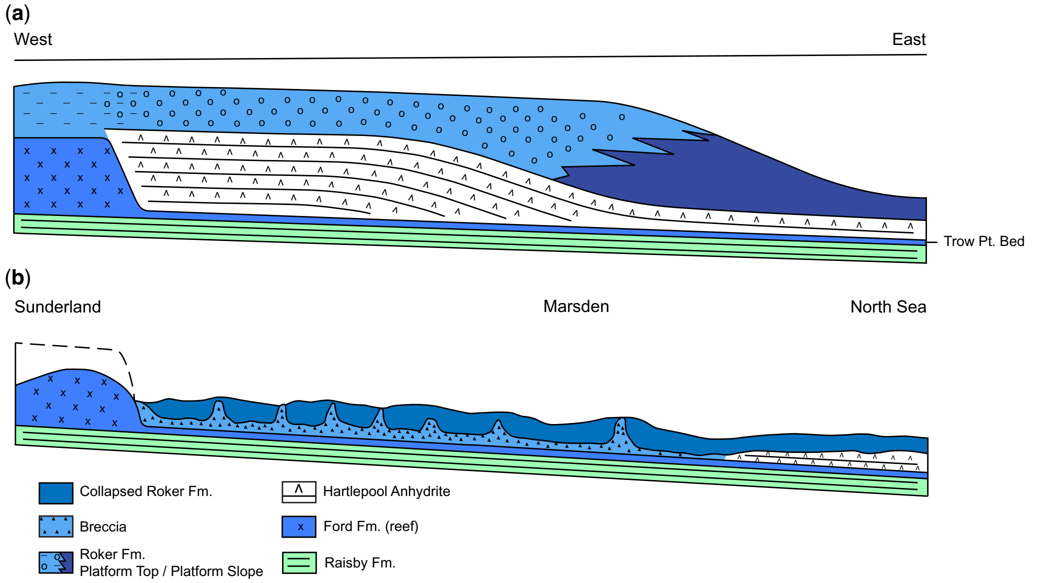

Fig. 4. (**a**) Schematic cross-section of Z1 and Z2 depositional lithostratigraphy across NE England (shading as in Fig. 1). (**b**) Schematic of present-day lithostratigraphy following dissolution of the Hartlepool Anhydrite in NE England (after Pettigrew 1980, with the permission of Durham Wildlife Trust).

succession has traditionally been subdivided into cycles (Figs 1 & 3); three carbonate–evaporite cycles in the lower part (Z1, Z2, Z3) and two thinner clastic–evaporite cycles in the upper part (Z4 and Z5) are distinguished in NE England (Smith *et al.* 1986). Further east in Germany and Poland, two more cycles can be distinguished (Z6 and Z7) (e.g. Doornenbal & Stevenson 2010).

A sequence stratigraphic interpretation has also been applied, based on lowstand evaporites and transgressive-highstand carbonates, recognizing seven sequences, ZS1–ZS7 (Figs 1 & 3) (Tucker 1991). Alternative sequence stratigraphic interpretations have been made in Germany and Poland and the Netherlands. Although Tucker (1991) regarded the Werraanhydrit as a lowstand evaporite and so the beginning of his third depositional sequence, an opinion supported by Warren (2006) in his review, Strohmenger *et al.* (1996) placed a sequence boundary in the middle of the Werra and interpreted the lower part as the highstand systems tract (HST) of the second sequence and the upper part as belonging to the next sequence. However, as the thick basin-centre Zechstein evaporites are likely to have formed when the Zechstein Sea was isolated or cut off, to a lesser extent (gypsum precipitation) or greater extent (halite precipitation), from the open global ocean, it is maintained that the major evaporite units (such as the Werraanhydrit) are best regarded as forming the lowstand systems tract (LST) of each of the sequences. The sequence boundaries and systems tracts recognized by Strohmenger *et al.* (1996) and others *within* these evaporite units are more likely to be the result of higher-frequency base-level changes within the Permian Basin and its sub-basins, in view of their disconnect from ‘global’ sea-level changes affecting the Permian Basin as a whole – that is they form parasequences within lowstand evaporites.

The complete Zechstein depositional succession in NE England is depicted in Figure 1. Figure 3 shows the stratigraphy for NE England and their equivalents in the North Sea and continental Europe, along with the abbreviations commonly used for the units and sequence stratigraphic interpretation (revised from Tucker 1991; GRL 2016). Following deposition, the Zechstein succession in the more northerly Durham Province was likely buried to a depth of several kilometres, as is still the case with equivalent strata in the Zechstein Yorkshire Province further south (i.e. in the Cleveland Basin), where Triassic up to Middle Jurassic sediments are preserved above the Permian (Słowakiewicz *et al.* 2015*b*). Preferential uplift of the Durham Province has been attributed to the presence of a low-density Devonian granite beneath the region (Kimbell *et al.* 2010): the outcrop is located on a structural high, the Alston Block. There is no definitive evidence for the timing of uplift of Zechstein strata in NE England but it is widely assumed that this took place in the late Cretaceous–early Tertiary (Smith 1972; Lee & Harwood 1989).

Zechstein stratigraphy and diagenesis

Zechstein cycle 1 (Z1) stratigraphy

In NE England, the first-cycle carbonates (Z1/Ca1) consist of two formations, the Raisby Formation, a distally steepened ramp deposit, and the Ford Formation, a reef-rimmed shelf carbonate (Fig. 1; Smith 1980). Together, they are equivalent to the Zechsteinkalk of the SNS and NW Europe (Fig. 3). The Raisby Formation (up to 75 m thick) comprises medium-bedded limestone–dolomite slope deposits, with local calciturbidites (Lee 1993). In the uppermost part of the formation there is a slide plane, upon which in many places sits a major slide deposit of megabrecciated Raisby Formation (the 'Down Hill Slide' of Smith 1970). Smith attributed the origin of the megabreccia to 'earthquakes' or synsedimentary tectonic movements, whereas Tucker (1991) ascribed the megabreccia to a sea-level fall and forced regression (falling stage systems tract (FSST), Figs 1 & 3).

The overlying Ford Formation reef (Ca1/Z1, equivalent to the upper Zechsteinkalk in the SNS and onshore Europe), formed a shallow shelf around the basin (Fig. 1). At Trow Point, a 10 cm-thick microbialite (the 'Trow Point Bed') overlies the irregular top surface of the megabreccia, and is interpreted as the condensed basinward equivalent of the 100 - m-thick Ford reef (Smith 1986). The Ford reef is exposed in outcrops west of Trow Point, closer to the Zechstein basin margin, for example at Claxheugh Rock, *c.* 10 km to the SW near Sutherland (Smith 1986; Figs 4–5). The Trow Point Bed consists of basinal deposits (stromatolites, oncoids and peloids) that can be traced throughout the Zechstein Basin (in the NPB as well as SPB), being recorded in many wells and present in the subsurface of Poland onshore (Smith 1986).

Hartlepool Anhydrite

The Hartlepool Anhydrite was deposited basinwards of the Ford reef, as a lowstand wedge some 20–30 km across, with a present-day thickness generally of *c.* 100 m but reaching 130 m (Figs 1 & 5) (Smith 1994). The evaporites were precipitated up to, or close to, the top of the reef, such that there was limited or no anhydrite deposition upon the reef itself to the west and hence no later dissolution/collapse brecciation of the overlying Roker Formation to the west in this part of the outcrop.

The Hartlepool Anhydrite is generally nodular, commonly with a chicken-wire fabric, but it may well have been selenitic gypsum originally, as recorded by the Werraanhydrit in Germany–Poland (Richter-Bernburg 1985). Lenticular to isolated stromatolites grading to beds of microbial laminite with interbedded gypsum do occur within the Hartlepool Anhydrite, especially in marginal locations, in offshore borehole cores, typically forming less than 10% by volume, but locally up to 50%.

The Hartlepool Anhydrite is not present at outcrop in the study area since it has undergone dissolution on exhumation (Smith 1994) (Figs 4 & 5). Dissolution of this anhydrite caused foundering and collapse of the overlying Roker Formation carbonates (Smith 1972). Smith (1994) estimated that 80–120 m of anhydrite was removed, based upon the thickness of evaporite encountered in local offshore wells (Fig. 5). The residue of the Hartlepool Anhydrite presently overlies the Trow Point Bed and is typically 1–2 cm thick at Trow Point (Smith 1995). The residue is significantly thicker (2 m or more) at Ryhope (near Sunderland, *c.* 6 km south of Trow Point), a locality closer to the basin-margin than Trow Point (Smith 1995). Smith (1972, p. 260) described the residue in outcrop as a 'grey brown irregularly laminated mushy deposit composed mainly of carbonate, clay minerals with some gypsum, quartz and traces of detrital heavy minerals'.

Zechstein cycle 2 (Z2) stratigraphy

The Roker Formation (Z2/Ca2; equivalent to the Hauptdolomit of the SNS and NW Europe) was deposited directly on top of the reef and across the evaporite platform in a shelf to slope carbonate system (Fig. 1). It prograded basinwards, towards the east into the SPB (Mawson & Tucker 2009). At outcrop in NE England, shallow-shelf to lower-slope facies are exposed. The shelf margin was now located further to the east, more basinward than the earlier Ford Formation margin due to the development of the earlier (and at this time still not dissolved) gypsum wedge (Hartlepool Anhydrite). The shallow-shelf facies typically consist of cross-bedded oolite with rare bioclastic debris. Stromatolites and microbialite buildups are locally interbedded with oolite (Perri *et al.* 2013). The upper slope facies of the Roker Formation consists of channelized graded beds (calciturbidites) and mass-transport deposits (calcidebrite and slide deposits). The lower-slope facies consists of interbedded thin calciturbidites and finely laminated hemipelagites (Mawson & Tucker 2009). The total Roker Formation thickness is estimated to be *c.* 100 m. On a large scale, the Roker Formation represents a single transgressive–regressive succession (TST to HST), but several orders of higher frequency cycles are recognized, likely formed through orbital forcing (Mawson & Tucker 2009). Of note at Marsden Bay, where the collapse breccias are well developed, is the presence

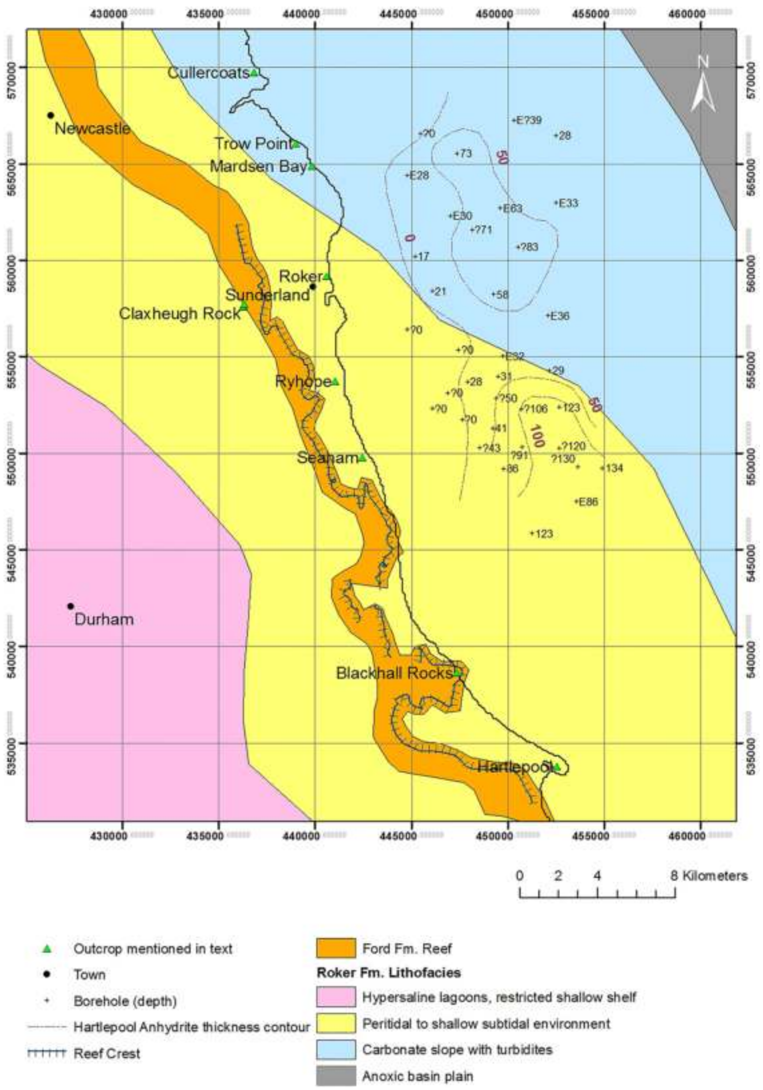

Fig. 5. Approximate present-day thickness of the Hartlepool Anhydrite offshore, NE England displayed with the Roker Formation facies in the background, and the Ford Formation reef shown in orange on top. Based on borehole thicknesses and outcrop observations (based upon Smith 1994, with the permission of the British Geological Survey), Roker Formation facies map and Ford Formation facies map adapted from Smith (1989, figs 7 & 9, by permission of the Yorkshire Geological Society).

of a distinctive unit, the 'Orange Marker', comprising clay-rich turbidites within lower-slope laminated facies: this represents a parasequence boundary.

Zechstein diagenesis

The diagenesis of the Zechstein carbonates is complex, but some background is provided here since some aspects are related to the deposition, mineralogical changes and dissolution of the evaporites discussed in this paper. Figure 6 summarizes the diagenetic processes involved in a time/depth framework. The Zechstein carbonates, oolitic and bioclastic grainstone, reefal and microbialitic boundstone, and lime mudstone (micrite) (Smith 1994) would have been deposited with a mixed mineralogy of aragonite, high-Mg calcite and low-Mg calcite, similar to modern carbonate sediments.

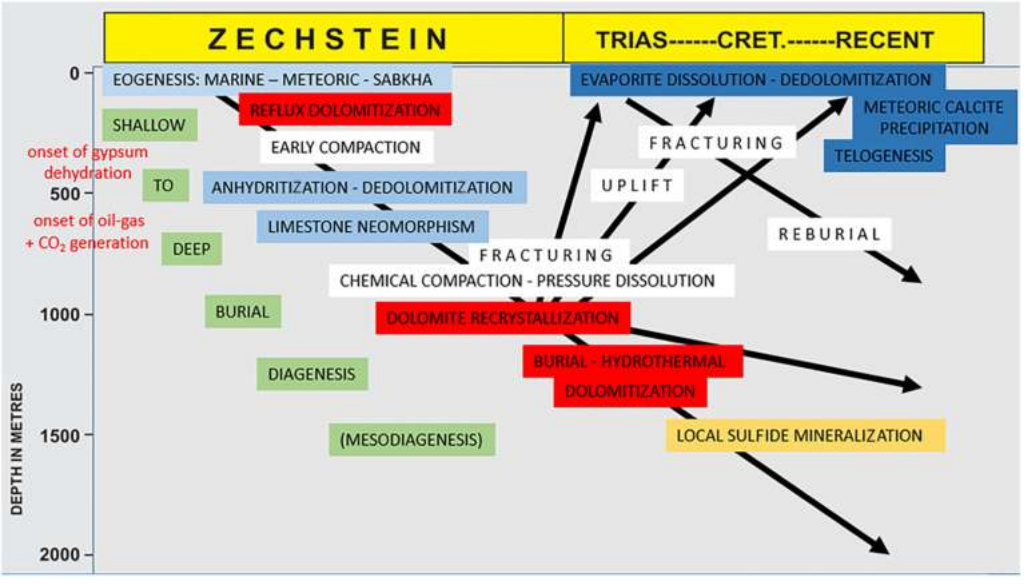

Fig. 6. Schematic diagram for the Zechstein carbonates showing the diagenetic processes involved in a depth and time framework.

Early marine cementation is recorded, as well as early meteoric dissolution–cementation, and sabkha – microbial dolomitization (Tucker & Hollingworth 1986; Perri *et al.* 2013; Słowakiewicz *et al.* 2015*a*). The majority of the Zechstein carbonates are pervasively dolomitized and this is thought to have occurred through a near-surface reflux process involving seawater and/or evaporated seawater (e.g. Clark 1980; Harwood 1986). Some original limestones avoided dolomitization, however, notably particular units of the Roker Formation (Z2) outer-shelf to slope facies, some with a distinctive nodular/concretionary fabric. Recrystallization (neomorphism) of original limestone has also occurred. In addition, dolomites have commonly been dedolomitized, i.e. calcitized and converted to a secondary limestone. This is considered to have taken place at two discrete intervals (discussed in more detail later): (1) during shallow-to-moderate to deeper burial, possibly through interaction with Ca-rich fluids derived from gypsum dehydration to anhydrite (as is the case in the Zechstein of Germany, Schoenherr *et al.* 2018); and (2) during uplift related to dissolution of gypsum–anhydrite, contact with meteoric water and formation of collapse breccias (Smith 1972). During burial, anhydrite was commonly precipitated in cavities and between grains as a cement, occluding porosity. On subsequent uplift and contact with meteoric water, this sulfate was dissolved out to form vuggy pores, a feature of many Zechstein carbonates at outcrop, and they may be lined or filled with calcite cement (Lee & Harwood 1989). Dissolution of gypsum–anhydrite would have taken place through contact with meteoric water on uplift as the strata came into the realm of fresh ground water. However, meteoric water could have descended into the subsurface along porous zones within limestones and sandstones, and down faults, where there is sufficient hydraulic head, and dissolve gypsum adjacent to those porous rocks or faults (thus meteoric water could have descended several hundred metres subsurface).

The collapse breccias of NE England

Roker Formation collapse breccias

The lower parts of the Roker Formation are well exposed in sea-cliffs, extending for over 3 km between Trow Point and Lizard Point, near South Shields, Sunderland, on the coast of Tyne and Wear (Fig. 7). The gentle regional dip is to the SE, such that the succession youngs southwards. The Roker Formation is not pristine here; it is collapse brecciated from the base upwards, where it overlies the residue of the Hartlepool Anhydrite (i.e. the horizon of evaporite dissolution). Overall there is a decreasing intensity of deformation as the vertical distance upwards from the residue increases.

Over a vertical sequence through the Roker Formation, there are several types of breccia represented

Fig. 7. Map of study area showing places named in text. ESRI World Imagery using Getmapping 1 m resolution imagery for Great Britain is used as a base image. Graticules spaced every 1 km.

(Fig. 8) that occur in three zones, as follows, in ascending order:

Zone A: A stratiform chaotic breccia (*c.* 13 m thick) at the base, where the sediments once rested on the underlying anhydrite.

Zone B: Highly fractured host rock (mosaic to crackle breccia), with rafts of bedded (i.e. unbrecciated) strata separated by fractures and local breccia bodies, overlying the stratiform breccia (*c.* 10 m thick).

Zone C: Host rock retaining primary fabric, with broad-scale open folding, faults and localized breccia development, with deformation decreasing upwards through the overlying Roker Formation.

Zones B and C also contain numerous steeply oriented breccia 'pipes', with a vertical extent of some tens of metres and diameter up to 30 m, as well as variably shaped breccia bodies that typically range in size from 1 to *c.* 10 m across.

Note that laterally to the south, for example at Blackhall Rocks, where the Roker platform directly overlies the Ford Formation reef, the Roker Formation is not brecciated, since, as noted previously, no anhydrite was deposited or subsequently dissolved on top of the reef, only basinwards of it (it is a lowstand evaporite).

Breccia terminology. A 'collapse breccia' is defined as a breccia formed by the brittle gravitational deformation of rock overlying an opening or cavity (based upon Gutiérrez *et al.* 2008). The term 'collapsed' used herein refers to the carbonate rocks overlying the dissolved evaporite which have been subject to gravitational deformation; this can also be termed foundering. The karstic breccia terminology of Loucks (1999) can be applied to these breccias. The collapse brecciation described herein all occurs within the Roker Formation; the collapse breccias in the overlying Seaham Formation are not described.

Zone A: Stratiform chaotic breccia

The stratiform breccias are exposed in the northern part of the study area, between Trow Point and

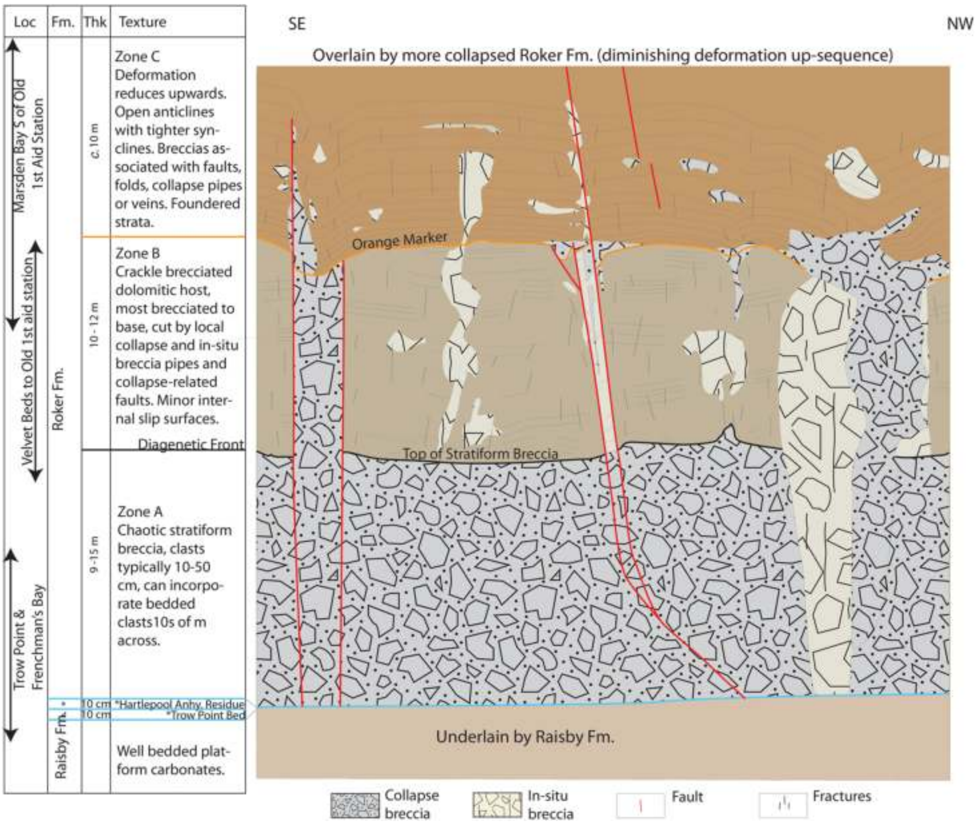

Fig. 8. Schematic depiction of the deformation associated with dissolution of *c.* 100 m of evaporite as observed in the cliffs from Trow Point along to Marsden Bay, across the lowermost collapsed Roker Formation. The Hartlepool Anhydrite was originally between the Trow Point Bed (which lies upon the Raisby Formation including the megabreccia) and the Roker Formation.

Velvet Beds (Fig. 7). The stratiform breccia is 10–15 m thick (Figs 8 & 9). The lower boundary rests directly on the Hartlepool Anhydrite residue, is sharp, planar but irregular (e.g. at Trow Point), with up to 1–3 m of relief inherited from the megabreccia deposit that underlies the Hartlepool Anhydrite Residue and also the Trow Point Bed. The upper boundary of the stratiform breccia grades into highly fractured Roker Formation (Zone B) across an approximately horizontal transition zone up to 1 m thick (Figs 8 & 10). Much of the stratiform breccia has been subject to extensive calcitization (dedolomitization). The upper limit of the calcitization is irregular and is referred to as the 'diagenetic front' (e.g. Fig. 8). The diagenetic front is broadly, but not always exactly, coincident with the top of the stratiform breccia. The breccia beneath the diagenetic front is generally much more resistant to weathering than the crackle breccia of Zone B and commonly forms prominent irregular exposures and headlands along the coast (Fig. 10).

Internally, the breccia has a massive structure, with open fractures that are commonly vertical to subvertical displaying typical lengths of 1 m or more. There are local slip surfaces and normal faults, as noted by Smith (1972). Vertical connectivity across this unit, via the fracture network, is inferred to be excellent, thanks to a relatively high intensity of well-interconnected 'longer' fractures (>1 m) and a relatively low intensity of small fractures. The relatively sharp base and more gradational top of the stratiform collapse breccia are typical features of collapse breccias, as is the stratigraphic position, above a horizon that is laterally equivalent to evaporites (Figs 1 & 8).

The stratiform breccia is mostly monomictic, clasts are dominantly dolomitic with some clasts of dedolomite/limestone, set within a calcite matrix (Fig. 9). The dolomite clasts in the breccia tend to weather out preferentially (thought to be a recent phenomenon caused by surficial weathering), resulting in a so-called 'negative' or 'cellular breccia'

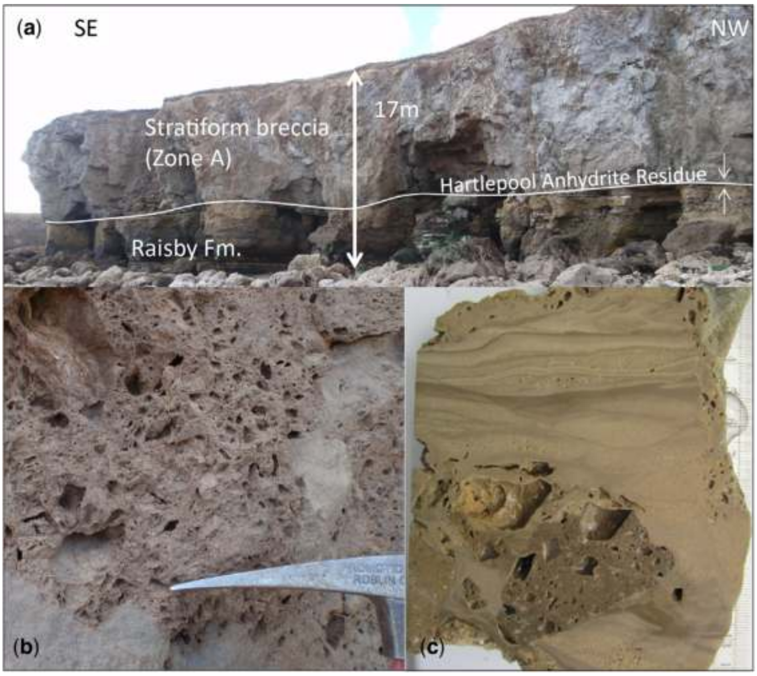

Fig. 9. Zone A: (**a**) stratiform breccia overlying the Raisby Formation at Frenchman's Bay. (**b**) 'Negative breccia' from the stratiform breccia at Trow Point (Lebour 1884, also called 'cellular breccia', Sedgwick 1829) in which the dolomite clasts have weathered out to leave the more resistant calcite matrix. (**c**) Slabbed hand sample from Trow Point of matrix-rich stratiform collapse breccia (sourced near the base of the stratiform breccia). Note the metal ruler for scale to the right of the image. Clasts of breccia lie within laminated/thinly layered sediment, the dolomite clasts have been dissolved out of the breccia (the clast is a piece of breccia). The laminae/layers show normal grading and were water-lain, deposited within cavities and caves as the evaporite was dissolving; they now occur as pockets within the collapse breccias (especially common towards the base of the stratiform breccia). Deformation associated with collapse continued while sediments were semi-lithified, some matrix porosity can be seen in the coarser sediments and vugs occur.

(Fig. 9b) (Sedgwick 1829; Lebour 1884, respectively). Up the succession, the number of clasts which are themselves fragments of earlier breccia increases, i.e. there is increasing evidence for multiple phases of collapse brecciation and cementation (Woolacott 1909, 1912; Smith 1972); collapse brecciation was polyphase. There are local relatively large rafts of bedded Roker dolomite within this stratiform breccia, reaching several tens of metres across. The breccia is clast supported, mostly unsorted, with blocky clasts typically from a few millimetres to 50 cm in diameter, although they show a wide range in size (Fig. 9b, c).

The matrix between clasts is finely comminuted carbonate ('rock flour'), grey-cream to tan-pale brown colour. The calcite matrix of the breccia is extremely hard; this is likely the result of recrystallization or dedolomitization/calcite cementation associated with the diagenetic front. Towards the base of the stratiform breccia, there are lenses of hard, strongly cemented silt to sand-grade calc-lithite. The lenses of matrix can be tens of centimetres to a metre or more in extent and commonly show planar and cross-lamination, small overfolds and deformed, contorted laminae (Fig. 9c), in places with small synsedimentary faults, indicating early lithification. Scattered centimetre-sized clasts tend to show an alignment of long axes. These laminae were clearly deposited by flowing water and must represent the development of subterranean streams within the dissolving mass of gypsum–anhydrite, the calc-lithite matrix having been reworked from the carbonates interbedded with the anhydrite and the collapsing overlying Roker Formation. Visual estimates of matrix porosity range from 0 to 15% (Table 1). Local listric fractures cut through the stratiform breccia with a tan brown-coloured matrix and clasts of stratiform breccia (for example at Trow Quarry, 100 m south of Trow Point).

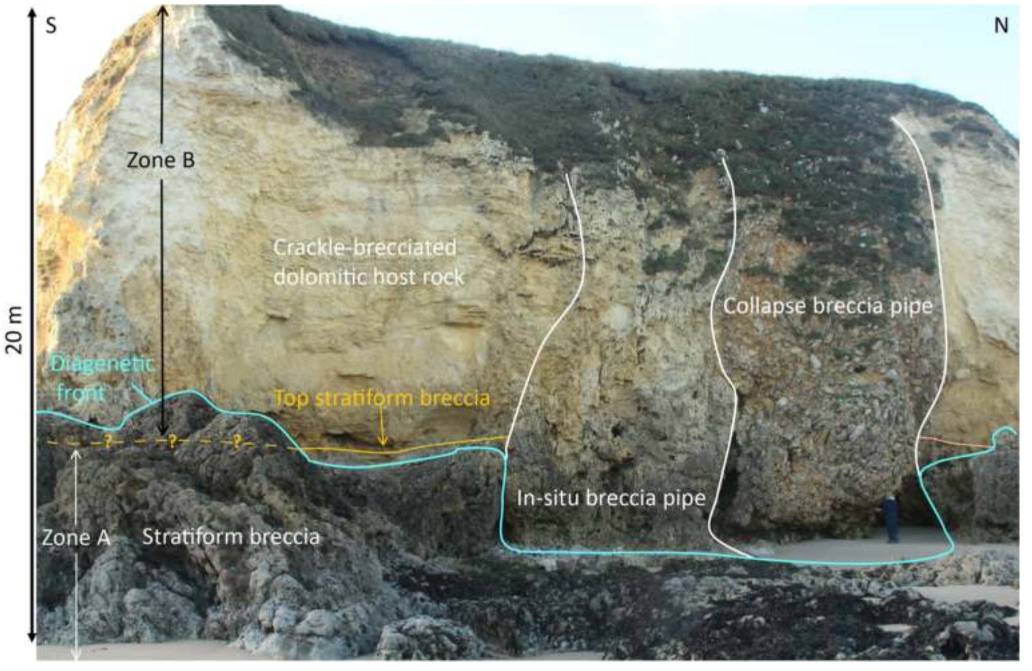

Fig. 10. Cliff section at Velvet Beds on the north side of Marsden Bay. The stratiform breccia of Zone A is visible to the base of the section, mostly below the diagenetic front, above which is Zone B. Breccia pipes are delineated, with the breccia pipe in the centre divided into two different components, *in-situ* breccia, locally exhibiting a cellular or negative breccia texture, and a collapse-breccia pipe, dominated by angular grey limestone clasts, a tan matrix with local alignment of clasts.

Zone B: highly fractured Roker Formation (mosaic to crackle breccia), with discrete breccia bodies

Zone B is exposed southwards from Velvet Beds to *c.* 30 m north of the old firstaid station, in the northern part of Marsden Bay. Overlying the stratiform breccia, Zone B is composed of buff-coloured dolomite that exhibits a laterally varying degree of brecciation (Figs 8 & 10). Typically, the rock is a crackle or mosaic breccia, i.e. the strata are fractured into a breccia, but the individual clasts exhibit consistent bedding and little or no relative displacement. Hence, on first inspection, the dolomitic host rocks appear to retain much primary bedding. Towards the base of Zone B the strata are broken up laterally and vertically into metre-scale clasts. Up-section, the size of the clasts increases. Fractures within Zone B can have a cream-coloured calcitic fill, or are apparently open, unfilled features. One sample of dolomitic crackle breccia had a visual estimate of porosity of 7% (Table 1).

At Velvet Beds, Marsden, the top of Zone B broadly coincides with the distinctive Orange

Table 1. *Visual estimations of porosity for the different features*

Zone	Feature sampled	Porosity range (%)	No. of samples
A	Stratiform breccia	0–15	2
B	Crackle breccia	7	1
C	Breccia associated with small faults/folds (<10 m)	1–4	2
C	Bed-bound breccia	7	1
B	Collapse-breccia pipe	1–15	3
B	*In-situ* breccia pipe	1–10	2
B and C	Fault breccia	0–32	7

Marker. From *c.* 30 m north of the old firstaid station, there is a lateral transition such that Zone C begins below the Orange Marker. This lateral variation in the degree of brecciation is another feature typical of collapse breccias. Unfortunately, the quality of the exposure here is low, obscuring the exact nature and location of the Zone B to C contact.

Zone C: host rock retaining primary fabric, with broad-scale open folding, faults and localized breccia

Zone C is well displayed southwards of the old firstaid station in the centre of Marsden Bay, in the coastal exposures further to the south to Lizard Point and then Roker. Above the crackle-brecciated Zone B, the heterogeneous limestone and dolomite succession is significantly less deformed (Figs 8 & 11). Primary bedding is preserved, although some localized breccia bodies do occur. Typically, beds are arranged in open anticlines occurring over 10–40 m and tighter synclines occurring over 2–10 m. Breccia commonly occurs beneath the synclines, suggesting that the folding was forced by local, gravitational processes, due to vertical collapse following underlying dissolution.

Other common features within Zone C include wide aperture open tensile fractures, which occur preferentially within limestones, typically with a stepped appearance when viewed at bed scale (Fig. 12b). Compressional features are widely found within a few metres of extensional features, for example the small thrust and fault propagation fold in Figure 12a. There is a spatial association between compressional structures and breccia, with breccia locally extending between compressional and extensional structures. Visual porosity estimates of 1–4% (Table 1) are given for the breccias associated with structures shown in Figure 12a, and 7%

Fig. 11. Examples of deformation within Zone C. (**a**) Fault-related collapse breccia towards the base of Zone C, south of the old firstaid station. Orange line is the Orange Marker, which is a mechanical boundary but not the boundary between Zones B and C here (further north at Velvet Beds the Orange Marker is the boundary). White lines depict breccia. Carbonates shown here are dominantly dolomitic, with limestone above the Orange Marker and local beds SE of the fault. (**b**) Breccia bodies within dolomite below the Orange Marker (darker unit above the Orange Marker is limestone). (**c**) View facing NNW at Whitburn Rocks. The cliffs in the background show mainly consistent primary bedding with local disruption. The dip of beds in the foreground can be seen to define a broad anticline and a tight syncline to the bottom right of the image. Note sailing boat for scale.

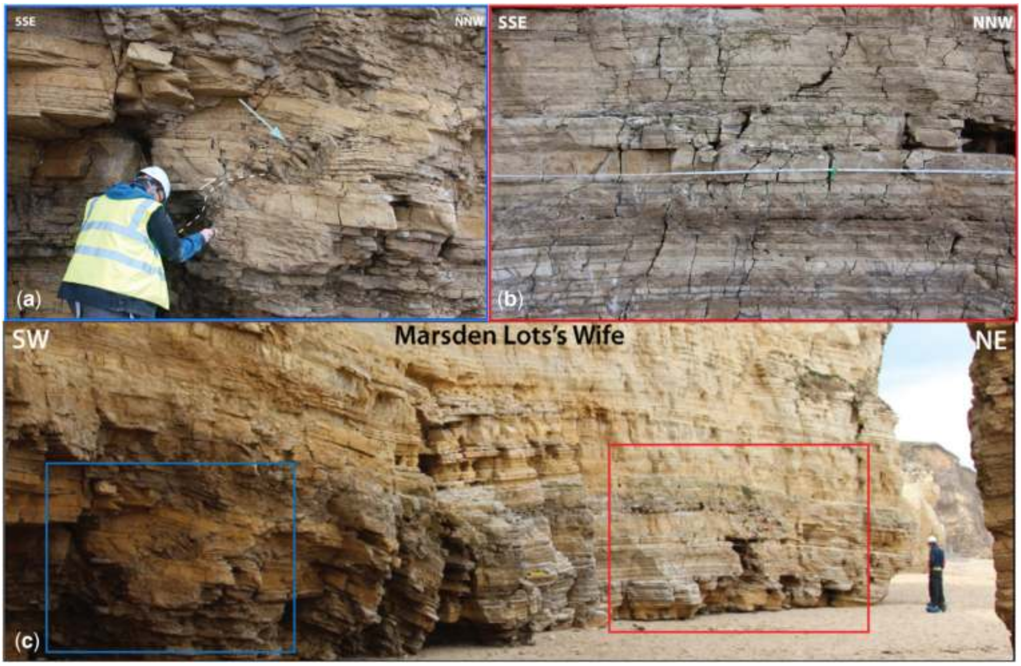

Fig. 12. (**a**) Small thrust fault and fault propagation folds. Limestone beds Zone C, Marsden Bay. Note the aperture creation as the fault propagation fold separates beds along mechanical boundaries (beds). (**b**) Wide aperture, unfilled fractures within limestone; note the stepped character of several fractures. (**c**) The blue box shows the location of (a): the red box shows the location of (b).

for the porosity of a bed-bound breccia extending between a compressional and extensional structure. The close association between local compressional and extensional (or tensile) fractures is typical of regions of gravity-driven deformation (Fossen 2016). In this case, the deformation is thought to be related to local collapse of the carbonate sequence following dissolution of the underlying evaporites.

Zone C continues up-section through the Roker Formation, becoming less disturbed upwards. Locally deformation extends up to the top of the Roker Formation, as displayed 15 km south of Marsden at Seaham Promenade, where narrow fractured/brecciated zones 2–15 m across occur, with beds either side dipping towards them, i.e. forming synclinal structures.

To the south of Lizard Point (and towards Roker), higher in Zone C than Marsden Bay, deformation becomes increasingly localized, with open anticlines extending up to 80 m across (a larger-scale syncline is reported south of this section at White Steel (Smith 1995), with fewer large breccia bodies (>10 m across) than further north and local intense fracturing (commonly spatially associated with large breccia bodies). There is still abundant evidence of disruption, but the bedding is generally more coherent at this level. Overall in Zones B and C, there is a reduction in breccia up-section, an increase in fold wavelength (anticlines become more open with much bedding appearing horizontal between synclines of 2–20 m across), and there are fewer faults and discontinuities and more contiguous bedding. In both Zones B and C, large breccia bodies (2 m across or greater) are observed to occur more commonly within host dolomite rather than within limestone units.

Collapse-related faults

There are several faults within Zones B and C, all of which have associated brecciation. Several NE–SW-oriented tectonic faults offset the Roker Formation at outcrop and extend down into the underlying Upper Carboniferous Coal Measures, as noted from mining records (Smith 1994). There are also multiple faults visible at outcrop that are not recorded in the mine workings and have several characteristics atypical of tectonic faults. They show steep to vertical dips bounding zones of brecciation commonly without a well-developed fault plane; the damage zone can expand downwards rather than away from the main slip surface; there is a relatively wide damage zone for any observed displacement and the breccias within the damage zone are chaotic, locally calcite cemented and, most importantly, display negligible tectonic fabric (Figs 11a & 13). The majority of these faults appear to be dilational, with small amounts of horizontal extension across them. These faults are interpreted to be related to collapse following evaporite dissolution, defining the edges of foundered blocks, and they are inferred to terminate downwards at the level of the Hartlepool Anhydrite residue and upwards within the collapsed sequence. Some breccias appear to be wedge-shaped and abut against collapse-related faults (e.g. NW corner of Marsden Bay, Fig. 13). Sampled visual matrix porosity estimates range from 0 to 32% for breccias along collapse-related faults (Table 1). Fracture corridors (narrow zones of increased fracture intensities with large vertical extent and connectivity) can occur proximal to these faults, commonly with highly fractured zones in local hanging walls.

Additionally, nearly all the tectonic faults that are noted to penetrate the underlying Carboniferous Coal Measures contain similar breccias to those in the steeper collapse-related faults at Permian outcrop level, and may have been reactivated during collapse.

Near-vertical breccia pipes

Visually the most arresting features of the Marsden Bay section through Zones B and C are the near-vertical breccia pipes. One particularly well-exposed breccia pipe extends up from the stratiform breccia at beach level and comprises two different components (Figs 8, 10 & 14):

(1) A cement-supported chaotic breccia spatially associated with a high density of near-vertical pale-yellow veins (Figs 14a & 15). This is interpreted to have formed *in situ* as is suggested from the gradational nature of the boundary between the host rocks, the mosaic, crackle and chaotic breccias of which the breccia is formed. There is a commensurate increase in pale-yellow vein intensity across the contact, the breccia was created by intense fracturing and veining. The light orange-yellow vein fill cross-cuts diagenetic sparry calcite concretions that partly overprint laminated original dolomite (Fig. 15c,d). The sub-vertical veins associated with the *in-situ* breccias appear to extend across the boundary between the stratiform and these overlying breccias, indicating that the veining postdates formation of the stratiform breccia. Visual porosity estimates range from 1 to 10%. For convenience, this unit is referred to below as the '*in-situ*' breccia.

(2) A clast-supported chaotic breccia, dominated by angular grey limestone clasts set in a distinctive cream to tan-brown coloured matrix, is interpreted to be a collapse breccia

Fig. 13. The green arrows point to wedge-shaped collapse breccias against collapse-related faults, in the NW corner of Marsden Bay. The v-shaped wedges, easily identified by the coloration of the Orange Marker, are especially common along the northern part of Marsden Bay (in Zone B).

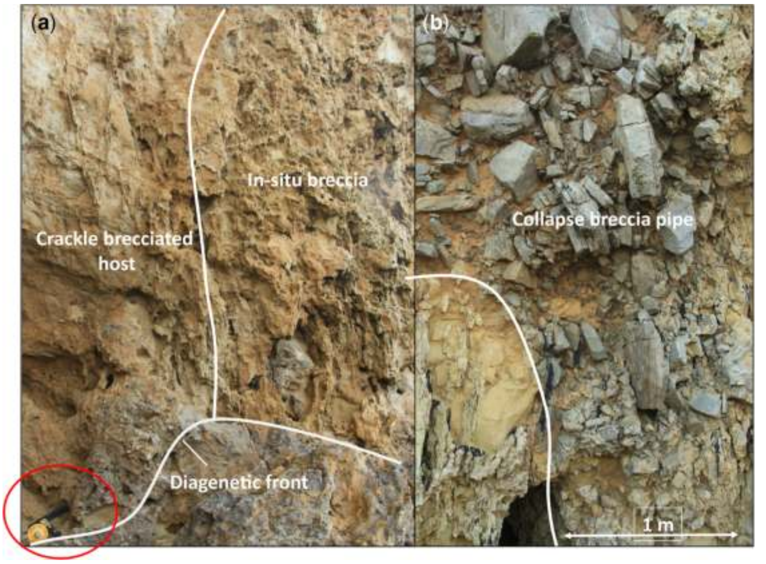

Fig. 14. (**a**) Close-up of the *in-situ* breccia, the (sub)vertical fabric of the pale yellow veins is visible. Note the exact margin of the *in-situ* breccia pipe with the host rock is gradational. Hammer for scale. (**b**) Close-up of the collapse-breccia pipe. There is a sharp contact with the *in-situ* breccia pipe, loosely aligned limestone clasts and distinctive tan-coloured matrix.

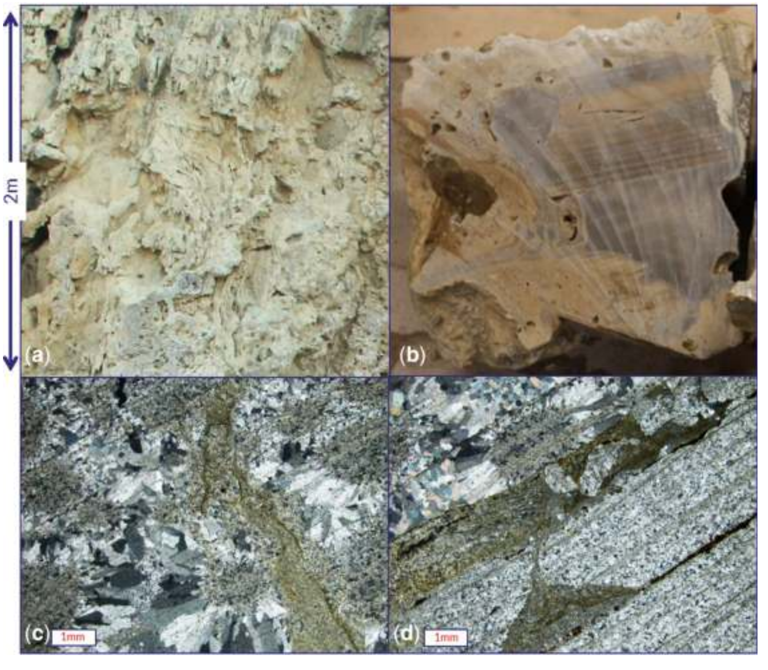

Fig. 15. *In-situ* breccia, with sub-vertical fabric forming outer part of breccia pipe seen in Figure 10. (**a**) Outcrop image with scale on LHS, note the sub-vertical fabric visible top centre. (**b**) Hand specimen showing finely laminated clasts set in brown matrix with small vuggy cavities and irregular laminae. (**c**, **d**) Thin sections in crossed polars. Both images show light orange-yellow matrix fills cross-cutting diagenetic sparry calcite concretions which themselves overgrow laminated original dolomite clasts. Note dark iron oxide rinds along clast-matrix contacts.

(Fig. 16). Within the collapse-breccia pipe, the clasts can display a weak alignment sub-parallel to the margins of the breccia body. The clasts are clearly derived from the limestone unit overlying the Orange Marker with rarer clasts of the *in-situ* breccia (Fig. 14). Cavities were filled by either deposition of remobilized sediment (with depositional laminae developed in some cases), local injection (possibly due to local overpressuring following collapse), or mineral precipitation (in some cases with geopetal fills, Fig. 16d). The fills between clasts are composed of iron-rich calcite cements with limonite/goethite, with vuggy porosity due to incomplete filling (Fig. 16). Mineral fills show distinctive cockade textures, associated with the evolution of iron-rich cement. This texture is indicative of an open-framework breccia and sequential precipitation at slow rates, of compositionally evolving cements around clasts which were commonly disturbed, rolled and rotated (Genna *et al.* 1996; Frenzel & Woodcock 2014). Visual porosity estimates range from 1 to 15%. For convenience, these breccias are referred to below as 'collapse-breccia pipes'.

The collapse-breccia pipe cross-cuts the *in-situ* breccia, indicating that the *in-situ* breccia formed prior to the collapse-breccia pipe (Fig. 10).

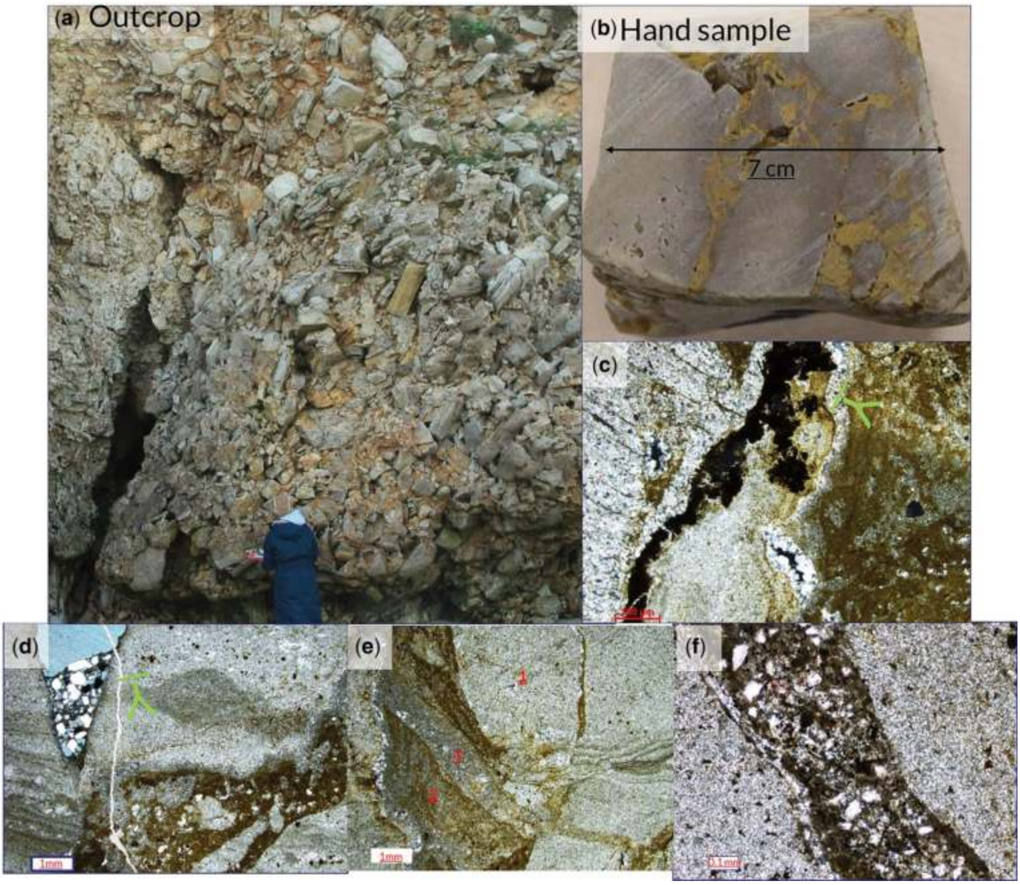

Fig. 16. Collapse-breccia pipe (**a**) in outcrop, note person for scale, and (**b**) in hand sample of collapse-breccia pipe seen in Figure 10 showing pale grey clasts and partially infilling brown matrix with large unfilled vuggy cavities some of which are lined with sparry calcite or black iron oxide. (**c**–**f**) Thin-sections of collapse-breccia pipe in crossed polars. Clasts are dominantly composed of calcite with a matrix of carbonate sediment plus sparse angular quartz grains (c–f). Multiple fills are preserved (e.g. fills 1–3 in (e)) with sparry calcite-lined vugs and geopetal structures giving way up (inverted Y pointing in direction of younging). Tensile fracture and dilation dominate; there is little evidence for significant clast abrasion or widespread hydrofracture.

Elsewhere, from Velvet Beds southwards into Marsden Bay, the *in-situ* and collapse breccias can be found both juxtaposed and spatially separated. The limestone unit immediately overlying the Orange Marker is the provenance of many of the clasts in the collapse-breccia pipes. It seems that the Orange Marker, with its elevated clay content relative to the surrounding carbonates, acted as a mechanical boundary close to the contact between limestone and dolomite units. The collapse-breccia pipes are interpreted to penetrate through the stratiform breccia, although clear examples of this relationship are not exposed.

Breccia textures

Regardless of whether the breccia bodies are located in pipes or beside collapse-related faults, there are some textural similarities for all breccias related to collapse: cockade textures, multiple iron-rich calcite cements, dominance of tensile fractures and dilation, and correspondingly little evidence for clast abrasion or hydrofracture (Fig. 17). The cockade textures indicate that the voids were open for long periods of time while the cements evolved compositionally and slowly precipitated, and some relative movement of the clasts took place during this time leading

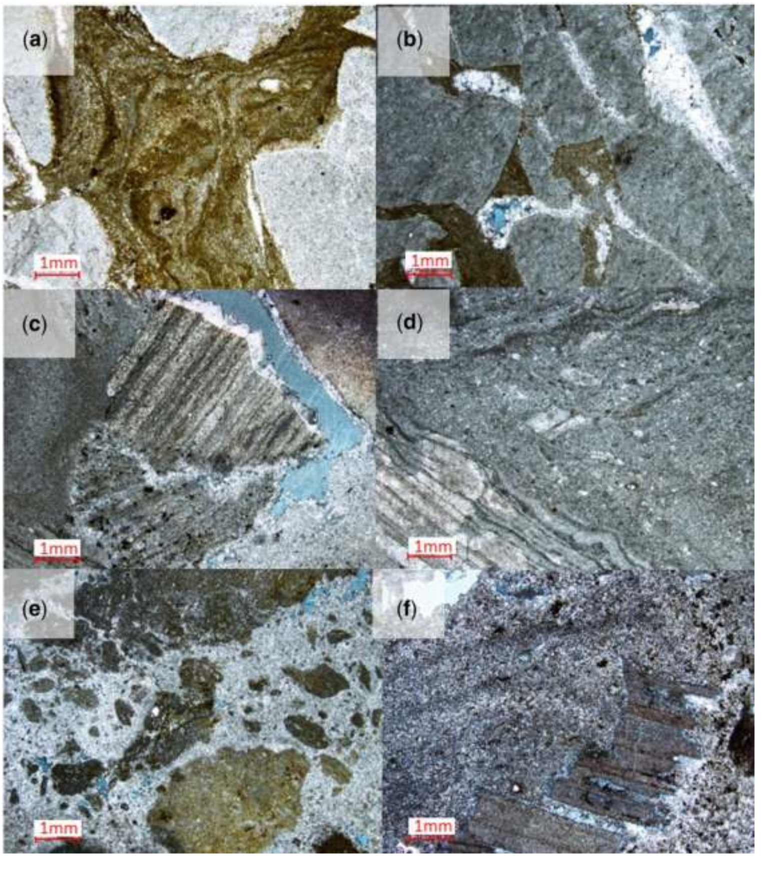

Fig. 17. Thin sections from variously sized breccia bodies sampled along Marsden Bay. Common features with all the breccias are early replacement of dolomite with calcite, multiple iron oxide and calcite fills which can be vuggy, varying amounts of clastic quartz, especially within the later fills, with little abrasion or attrition. Texturally these breccias are indistinguishable; however, the larger breccia zones typically have more polyphase fills and exotic quartz clasts in the matrix. (**a**, **b**) Thin sections of breccia from a large, non-tectonic breccia body: (a) calcite clasts with brown iron-oxide and calcite cement exhibiting cockade texture, (b) sparry calcite-lined vugs, geopetal structures. (**c**, **d**) Thin sections from an intermediate sized breccia body: (c) laminated clasts (originally dolomitic) lined with sparry calcite, vuggy porosity, (d) matrix fill of poorly sorted angular sediment. (**e**, **f**) Thin sections from a small breccia body associated with a small thrust fault: originally dolomitic clasts have been replaced with calcite, sediment matrix. All images in PPL, with blue resin, (f) stained for calcite (such that calcite is pale pink).

to them being enveloped in the cements. The larger breccia bodies more commonly have polyphase fills and exotic detrital quartz grains in the matrix compared to smaller breccia bodies, suggesting that they were better connected to external sources of clastic material, above or below (Fig. 17). These observations imply that the larger breccia bodies must have been open over large vertical extents, at least across the whole thickness of the Roker Formation, perhaps as far as the overlying Triassic sediments or even to the surface to allow ingress of exotic material (quartz grains).

Estimation of permeability within the observed sequence

Higher porosities occur consistently in the matrix and cavity fills; vugs and clast dissolution are common. Dedolomitization and clast dissolution lead to porosity generation, but not always with a high level of interconnectivity (i.e. relatively low permeability). The stratiform breccia of Zone A will likely have greatly enhanced matrix, vertical and lateral fracture permeability compared with an undisturbed Roker Formation slope succession (albeit this might not be the case for strongly cemented breccias). In addition to removal of a regional seal, the contrast between vertical and horizontal permeabilities within the carbonates is likely to have been reduced (i.e. k_v/k_h is anticipated to be larger after collapse).

Zones B and C are anticipated to have improved permeabilities, estimated to be half to a quarter of the typical Zone A matrix permeability, with a similar reduction in fracture permeability. Zones B and C are both cut by vertical breccia bodies with relatively enhanced permeabilities; the breccia pipes and collapse-related faults could act as conduits and themselves have matrix properties akin to the stratiform breccia. With regard to fracturing, the collapse-related faults when compared with the stratiform breccia typically have an increased intensity of small fractures and a lower intensity of larger fractures with lengths of 1 m or more. Additionally, they can have associated vertically extensive fracture corridors. Thus, the breccia pipes and collapse-related faults can transmit fluids along their lengths more rapidly than the host rock, but less rapidly than the stratiform breccias. Fracture corridors on the other hand have the potential to transmit fluids as rapidly as the stratiform breccia.

In summary, complete evaporite dissolution of the Hartlepool Anhydrite and collapse of the overlying Roker Formation results in increased matrix and fracture permeability of the carbonates, throughout the lowermost zone (Zone A). The overlying Zones B and C will have vertical conduits that are anticipated to flow at slightly slower rates than Zone A.

Diagenesis and isotope geochemistry of the collapse breccias

Associated with the widespread evidence for fluid circulation described above, the collapse breccias show a range of diagenetic effects related to the dissolution of the evaporites. Stable isotope analysis has been undertaken in order to unravel these diagenetic processes. The Roker Formation, the host rock of the breccias, is composed of dolomite and limestone. The limestone occurs as three types: (1) primary (i.e. mostly micritic calcite, textures well preserved); (2) recrystallized limestone; and (3) dedolomite. The last two are composed of moderately to coarsely crystalline, equant, fibrous and concretionary-nodular calcite, some with relics of original texture (e.g. lamination). Within the breccia there are clasts of these four rock-types (i.e. dolomite and the three types of limestone) and the matrix is derived from comminution of the host rock. The nature of the clasts in the breccia depends on which level of the Roker Formation was collapsing at the time. The collapse breccias vary from those with little alteration to those that have been completely recrystallized/dedolomitized. In addition, the space between and within clasts in the breccias are partly to completely filled with matrix, internal sediment, calcite cements and rarely other minerals.

In the matrix of the least-altered breccias, and the sediment of the laminated lenses that occur towards the base of the stratiform breccia, there has been little if any recrystallization; comminuted carbonate fragments are clearly visible set in a micritic sediment. However, in most cases the mineralogy of the matrix is calcite, which would indicate that any dolomite fragments have been dedolomitized. The fine matrix/sediment is well cemented, presumably by calcite. At outcrop, especially in the stratiform breccia, as noted above, dolomite clasts are commonly weathered out.

In its upper part, well seen at Velvet Beds, the stratiform breccia is commonly entirely calcitic in composition. The 'diagenetic front' (approximately coincident with the top of the stratiform breccia) can be considered a dedolomitization/calcitization front with the overlying dolomite (Figs 8 & 10). The limestone here is composed of a mosaic of fine to coarse calcite crystals, with ghosts of the original clasts, that is formed due to recrystallization of micritic matrix and limestone clasts to a mosaic of coarser calcite crystals, and dedolomitization of any dolomite clasts. The typical dedolomite texture of calcitized dolomite rhombs is not observed, likely since the original dolomite was fine-grained. Nevertheless, small rhomb shapes (<5 μm) are present within the coarse calcite replacing presumed dolomite.

Calcite crystals that occur within vugs in the clasts and between clasts where there is no matrix commonly show several phases. An earlier calcite generation of bladed to equant crystals lines cavities in an isopachous manner and a later phase of coarser drusy calcite spar fills cavities partly to completely. The earlier cement tends to be luminescent, whereas later phases are non-luminescent (Lee & Harwood 1989).

The various types of carbonate in the breccias and host rocks have distinctive $\delta^{13}C$ and $\delta^{18}O$ values reflecting their diverse origins. Zechstein dolomites from NE England generally have very positive $\delta^{13}C$ values between +5 and +6‰ and $\delta^{18}O$ values which range from near-zero to quite negative (−5‰) (Fig. 18; Clark 1980; Aplin 1981; Lee 1993, 1994). The high positive values of $\delta^{13}C$ are typical of Zechstein marine carbonates and reflect the high organic productivity of the Permian Basin. The low positive to near-zero $\delta^{18}O$ signature is consistent with precipitation from seawater or evaporated seawater, and the trend to more negative values is a reflection of dolomite recrystallization during burial. Primary limestones, as occur in the underlying Raisby Formation (Lee 1993) and locally in the Roker Formation, have $\delta^{13}C$ ranging from +5 to +6‰ and $\delta^{18}O$ from −2 to −5‰. The interpretation of these is similar to that for the dolomites: marine $\delta^{13}C$ and seawater $\delta^{18}O$ to depleted values through burial recrystallization.

Within the outer-shelf facies of the Roker Formation, concretions up to 30 cm in diameter are developed (e.g. the locally named 'Cannonball limestone') that typically consist of equant to fibrous calcite crystals, with vestiges of the bedding passing through them. These concretionary limestones have $\delta^{13}C$ varying from a marine value of *c.* +6‰ to less positive values of around +4‰. $\delta^{18}O$ varies from low negative values of 0 to −2‰, probably an original marine signature, to −4 to −6‰ (Fig. 18). The isotopic data support formation of these secondary limestones from shallow to moderate burial depths through neomorphism of an original mixed-mineralogy sediment to calcite. Dedolomite that formed during moderate burial, i.e. before uplift and evaporite dissolution, is well documented from the subsurface in Germany (Schoenherr *et al.* 2018) and occurs in the Roker slope facies at Marsden. The $\delta^{13}C$ values for this dedolomite range from +6 to +5‰, and the $\delta^{18}O$ values from 0 to −4.0‰ (Fig. 18). These data for the dedolomite are consistent with replacement of dolomite by calcite during moderate to deeper burial. It is thus envisaged that limestone recrystallization, dolomite recrystallization, dolomite calcitization (dedolomitization) and the neomorphism of carbonate to form concretionary limestone all took place during burial at shallow to moderate to deeper depths at increasing temperatures. A possible driving mechanism for these processes is the dehydration and dewatering of gypsum on its conversion to anhydrite, which can begin at a few hundred metres and continue to around 1000 m (Jowett *et al.* 1993; Schoenherr *et al.* 2018).

Dedolomitization of the collapse breccias, of reefal facies at the top of the underlying Ford

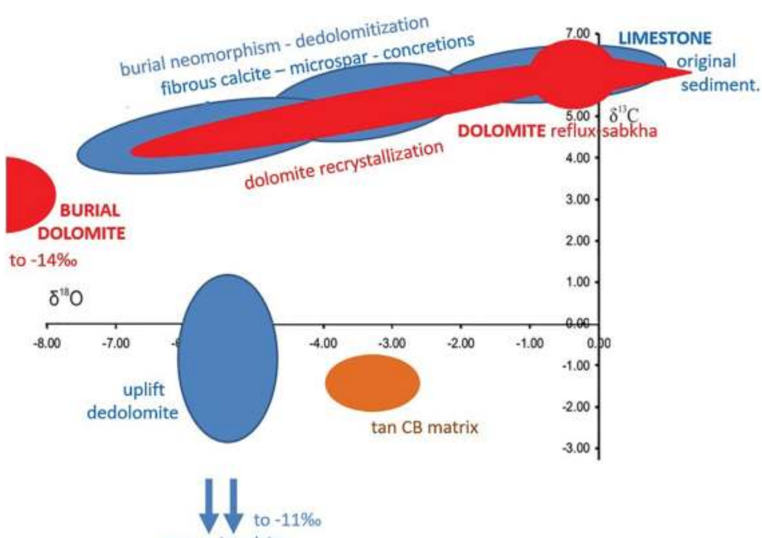

Fig. 18. Schematic cross-plot of stable isotope data for the Zechstein carbonates of NE England, based on analyses for this project and on data from the literature: Clark (1980), Aplin (1981), Lee (1993, 1994).

Formation, and also in platform facies at the top of the Roker Formation, immediately below the residue of the Fordon Evaporite – that is dedolomites which are directly associated with the evaporite dissolution, yield completely different isotopic signatures from all the other carbonates. $\delta^{13}C$ ranges from +1 to −3‰ and $\delta^{18}O$ values from −4.6 to −6.2‰ (Fig. 18). The tan-coloured matrix of the pipe breccias has similar values: average $\delta^{13}C$ −1.5 and $\delta^{18}O$ −3.9‰. The low positive–low negative $\delta^{13}C$ values plus low–moderate negative $\delta^{18}O$ of these collapse breccia-related dedolomites are consistent with alteration by meteoric water and are typical of dedolomites related to subaerial exposure at or near to regional unconformities (e.g. Cantrell *et al.* 2007; Hauck *et al.* 2018). Late diagenetic calcite cements within cavities after dissolution of sulfate, described by Lee (1993, 1994), have $\delta^{18}O$ signatures (−5 to −6‰) similar to these dedolomites, but $\delta^{13}C$ are more negative at −7 to −10‰ (Fig. 18), reflecting a greater effect of ^{13}C-depleted soil CO_2.

Discussion

The Zechstein sulfates were mostly deposited as gypsum, selenitic gypsum in particular, precipitated in shallow hypersaline lagoons, but also nodular gypsum formed in sabkhas, some of which may have been precipitated as anhydrite, as is seen in Abu Dhabi today (Kirkham 2011; Kirkham & Evans 2019). On burial, all gypsum would have been converted to anhydrite below several hundred metres. On uplift the anhydrite was converted to gypsum, with the hydration starting as meteoric water percolated down fractures and faults (e.g. Cooper 1986). In coal exploration boreholes located just off the NE coast of England, close to the outcrops discussed herein, the Hartlepool Anhydrite commonly shows evidence for rehydration (wholesale replacement of anhydrite by gypsum and/or alabastrine crystals within the anhydrite) adjacent to interbedded carbonate units and stringers as well as the top and base of the formation (M. Mawson pers. obs. and Smith 1994). Closer to the surface, the gypsum itself would dissolve adjacent to similar features and lead to the development of caves and cavities and collapse of overlying strata (e.g. Paul 2014).

Calcitizing fluids are believed to have been present within the evaporite and overlying Roker Formation throughout all stages of the collapse process following evaporite dissolution. Meteoric water likely became calcitizing through dissolution of the gypsum (as described by Schoenherr *et al.* 2018), and then passed upwards through the overlying Roker Formation.

Relative timing of events

The outcrop, thin-section and isotope evidence can be combined to reconstruct the following sequence of events, some of which likely overlapped (Fig. 19).

Stages 1 & 2. Dissolution of the gypsum was initially focused around pre-existing fracture networks and carbonate beds along which cavities and caves formed (Stages 1 and 2). The overlying carbonate beds fractured and collapsed into the void.

As the breccia gradually accumulated through roof collapse, some finer-grained sediment was deposited from subterranean freshwater streams flowing through the lower part of the developing breccia. As the lateral and vertical extent of the caves increased with progressive dissolution (Stage 3), the carbonates locally dipped towards the breccias. There were some episodes of re-brecciation as evidenced by the occurrence of clasts of breccia, indicating the further collapse of previously formed cavities, possibly as they became enlarged to some critical size or due to the dissolution of pods of anhydrite, as suggested by Smith (1972).

Zone A was only partly brecciated by Stage 3 and Zone B was little deformed at this stage, with localization controlled by fracture and fault networks, and minor, gentle folding overlying earlier-formed collapse breccias.

To explain the observed vertical zonation within the collapsed Roker Formation, we suggest that mechanical boundary layers controlled the vertical extent of the zones (e.g. Cooke *et al.* 2006). Such layers will act to retard the development of fractures and thus of breccia. It is likely that there was also a permeability contrast across such a layer, with possible pooling of fluids (and associated brecciation) below the boundary. The few fractures that do penetrate through such a mechanical boundary will have served to channel the calcitizing fluids into fewer conduits above the layer than below. This will have an effect of localizing deformation above mechanical boundary layers, compared with more diffuse deformation below. Mechanical boundary layers might have had higher clay or evaporite content, for example. The relatively clay-rich Orange Marker clearly acted as a mechanical boundary, as it appears to mark the boundary between Zones B and C in the vicinity of the Velvet Beds locality.

Calcitizing fluids circulated pervasively within the breccia within Zone A. They continually flushed through the stratiform breccia throughout the collapse process, lithifying the breccia quickly after it formed, dedolomitizing the clasts and matrix and re-lithifying the breccia after subsequent re-brecciation. Thus, the fluids cemented as well as replaced the clasts and matrix, i.e.

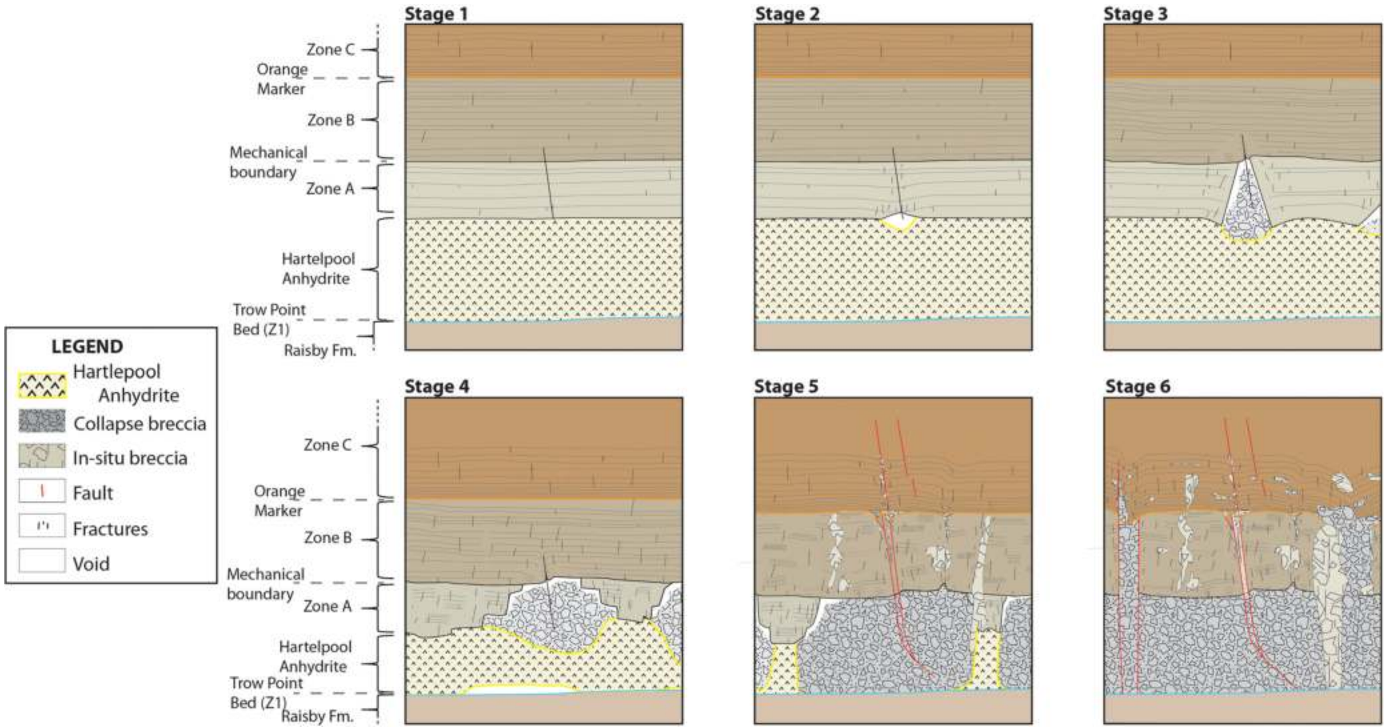

Fig. 19. Schematic diagram explaining the relative timing of the deformation observed at outcrop. See text for full explanation. This diagram does not show the whole of the Roker Formation, only the lower *c.* 40 m.

calcitizing or dedolomitizing the breccia. The position of the diagenetic front is thought to reflect higher permeability across the stratiform breccia, with local calcitization above the stratiform breccia exploiting higher permeability features.

As dissolution continued into Stage 4, the collapse of overlying Roker Formation into voids became more extensive in Zone A and the deformation progressed higher into the overlying section, with step changes in the degree of development across mechanical boundaries. Within Zone A, chaotic breccia bodies extended downwards below the original base of the Roker Formation at a level that formerly contained evaporite, focused around the fractures and faults along which early dissolution occurred. Above thicker remnants of evaporite, the Zone A strata were intensely fractured in Stage 4. As the amount of evaporite below Zone A continued to decrease by dissolution, the overlying Zones B and C began to founder, moving vertically with limited internal deformation.

The pale yellow sub-vertical calcite veins created the *in-situ* breccias in Zones A and B. Reductions in confining pressures due to ongoing exhumation and collapse allowed vertical and bed-perpendicular veins to form (as observed in Menezes *et al.* 2019). As the collapse deformation migrated up-section, so the level at which veins could form also extended upwards. The highest intensity of veining is thus in the lower zones, although veins are commonly hard to recognize within Zone A as they were then brecciated.

As evaporite dissolution continued, the deformation was further developed in Zones A and B, with the folding and fracturing initiating further up-section in Zone C (Stage 5). The presence of interbedded carbonates within the Hartlepool Anhydrite may have led to dissolution taking place at several levels contemporaneously. As dissolution progressed and voids coalesced there would have been the potential for large cavities to be formed locally under the collapsing Roker Formation. Accommodation of the larger vertical movements might have prompted the collapse-related faults visible in Zones B and C, where strain was localized, commonly along the edges of relatively undeformed blocks. The previously described clasts within Zone B that increase in size upwards are thought to reflect internal deformation within larger foundered blocks, rather than being separate foundered blocks themselves (inferred from the very closely aligned bedding across multiple blocks). The smaller block size towards the base indicates there was more deformation accommodated at the bottom of Zone B than at the top, possibly indicative of the whole of Zone B having foundered in one block at Velvet Beds. *In-situ* breccia pipes continued to form as the local concentration of pale-yellow calcite veins increased.

In Stage 6 collapse-breccia pipes, collapse-related faults and *in-situ* breccia pipes formed. The stratiform breccia was completely developed by this stage. Brecciation continued in Zone B, with local brecciation and folding in Zone C developing further. The listric fractures with tan-coloured matrix in the stratiform breccia are late-stage as evidenced by the matrix fill and could have been contemporaneous with the collapse-breccia pipes (possibly even with a direct genetic link).

Two main scenarios for formation of the observed collapse-breccia pipes are suggested:

(1) The margins of foundered blocks are thought to have been zones of high permeability and therefore increased fluid flow, which then led to further dissolution to create collapse-breccia pipes.

(2) Remnants of evaporite which were late to dissolve, acted as pillars, structurally weakening the overlying carbonate, and once then dissolved, formed approximately circular voids, that in turn were filled with collapse breccia.

Passing up-section within the Roker Formation, the number of breccia pipes decreases, with a few extending across the full thickness of the Roker Formation and possibly beyond to overlying units or even the palaeosurface. This connectivity is indicated by the local preservation of clastic sand grains found in some of the larger breccia bodies. The dissolution to create the pipes was likely a gradual process, but the collapse of overlying roof rocks could have been catastrophic, with later gradual mineral and finer-grained sediment fill. While these collapse breccias formed, the dissolution of the Hartlepool Anhydrite continued as indicated by the changing mineralogy of the cockade-textured cements within the collapse breccias. The mixture of matrix and cements within the collapse breccia indicates the slow nature of the fill.

The tan-coloured sediment within the collapse-breccia pipes is postulated to have been sourced from the carbonate components of the evaporite residue reflecting fluid communication from the base of the Hartlepool Anhydrite to the Roker Formation. The late-stage collapse-breccia pipes would have preserved high permeability, acting as conduits for transmission of late-stage fluids. The interbedded carbonates would have been less soluble than the evaporites, forming a residue some of which might have been mobilized increasingly as evaporite dissolution reached completion.

Gypsum dissolution rates of around 1 mm a^{-1} are reported in caves (Klimchouk *et al.* 1996;

Klimchouk & Aksem 2005) although higher rates of 0.04 to 1.7 m a^{-1} are reported for dissolution of Zechstein gypsum in the River Ure, Yorkshire (James *et al.* 1981). An evaporite thickness of 100 m would require 100 000 years to dissolve at the rate given for caves, although the presence of interbedded carbonates would likely modify this timespan.

Absolute age

There is no precise evidence for the timing of Zechstein uplift and dissolution in NE England. It has commonly been assumed that after burial to several kilometres, uplift took place in the late Cretaceous–early Tertiary (e.g. Lee & Harwood 1989). Apatite fission-track (AFT) data have been interpreted to indicate uplift and erosion of northern England on a scale of kilometres at *c.* 60 Ma ago (e.g. Green 1986). This might be related in some way to the kilometre-scale basin inversions that are recorded from the Cleveland Basin in Yorkshire, and the Sole Pit and Broad Fourteen basins in the North Sea to the SE at this time (Zeigler 1981). In addition, the early Cenozoic is known as a time of uplift and regional emergence across much of Britain (Lovell 1984). More recent workers have suggested that multiple episodes of exhumation occurred, including an additional Neogene phase. Monaghan *et al.* (2017) reported Cenozoic uplift for the offshore Cleveland Basin from Vincent's (2015) basin modelling, which varies across the MNSH. Hillis *et al.* (2008) recognized Cenozoic exhumation focused on compressional structures and an additional regional component of Paleocene exhumation in northern and central England and the SNS. Green *et al.* (2018) suggested exhumation between 22 and 15 Ma, and Fyfe *et al.* (2003) recognized Miocene and Pliocene/Pleistocene exhumation around the margins of the North Sea.

The Zechstein carbonate factory was formed close to sea-level and the carbonate platforms were exposed soon after deposition when sea-level fell and evaporites were precipitated around the basin margin against the carbonate slope (Z1 Hartlepool–Werraanhydrit) and within the basin itself (Z2 Fordon–Stassfurt Evaporites; Tucker 1991). Late Permian faulting has been recognized in the Netherlands, with contemporaneous subsidence in the UK Silver Pit Basin (Geluk 1999). East–west faults in NE England are known to have controlled the Z1 reef location and could have been reactivated prior to Z2 anhydrite deposition (i.e. during or after Z2 carbonates equivalent to the Roker Formation). Subaerial exposure causing dissolution-collapse during sea-level lowstands in Zechstein times is invoked as one possible cause for ovoid depressions mapped across the Z2 platform in the SNS. An alternative favoured hypothesis suggests a link to dissolution of halite pods although the two causes are not mutually exclusive (Grant *et al.* 2019). In the UK CNS, the Argyll Field (30/24) reservoir has been subject to collapse following evaporite dissolution; however, only 2 km away the Duncan Field and 15 km away the Innes Field have not been subject to collapse, but have intact reservoirs, implying there was no regional early dissolution and brecciation in the CNS. Strohmenger *et al.* (1996) cited evidence for sea-level fall immediately prior to and during development of the Z2 carbonate platform, which caused karstification of both the A1 anhydrite and the Z2 carbonate in Germany. Evidence for karstification has not been reported for this time in NE England, for example within the platform facies of the Roker Formation exposed at Blackhall Rocks. Nevertheless, this could have had an impact around palaeohighs elsewhere in the basin. In addition, at the end of the Permian, when the Zechstein Basin was filled with sediment, there may well have been an extended period of subaerial exposure, especially in the marginal parts of the basin, before deposition resumed in the Triassic. Evaporite dissolution could thus have occurred soon after deposition and/or at the end of the Permian and/or during late Cretaceous–Tertiary uplift. Local or regional climate variations may also have been significant. Higher rainfall further northwards in the NPB (at a higher subtropical palaeolatitude), compared to the SPB (Sorento *et al.* 2018), may have promoted the earlier (shallow burial) brecciation in the NPB; collapse brecciation in the Auk and Argyll fields appears to have occurred by Jurassic times.

Smith (1994, 1995) and Smith & Francis (1967) described ochre and red mudrock in the matrix of collapse-brecciated Seaham Formation (Z3) at Blackhall Rocks and Seaham and it is found at other localities (Figs 1 & 7). It is likely that this was sourced from the Roxby Formation at the top of the Zechstein which may extend up into the Triassic (Fig. 1). If the complete dissolution of the Fordon Evaporites and Hartlepool Anhydrite are temporally related this could serve to constrain the dissolution as being post-Zechstein, aged from Triassic times onwards. Isotopic constraints on the diagenesis within the collapse-brecciated Roker units indicate that meteoric water was likely involved, and that this occurred during exhumation following burial. The observed detrital quartz grains within the larger breccia bodies could then have been sourced from Quaternary deposits near surface, or from once-overlying Triassic Sherwood Sandstone. Smith (1972) recognized clasts of Sherwood Sandstone in some of the breccia pipes. Both a Triassic and surface source for the detrital grains are consistent with evaporite dissolution occurring when evaporites were in contact with meteoric water, as discussed previously. The Triassic Sherwood Sandstone is estimated to have been *c.* 220 m above the base of the Roker Formation (Smith 1972); thus Smith suggested the breccia pipes must have formed at depths greater than 200 m. The Sherwood Sandstone clasts would constrain the timing of formation of breccia pipes to be during or after the Triassic.

Near Whitburn, the Hebburn (or Monkton) dyke, part of the Tertiary Mull dyke swarm, appears to have been intruded into already-brecciated country rock, based on the dendritic shape of the dyke (Smith 1995). This provides the best evidence available at present to establish the age of the collapse breccias; the dyke swarm has been dated to about 58 Ma (Evans *et al.* 1973; Musset *et al.* 1988), indicating that dissolution of the anhydrite is constrained to being Paleocene or older in this area. These ages are consistent with a late Cretaceous– early Tertiary age of dissolution, but they do not rule out the possibility of earlier brecciation.

The spatial coincidence of the evaporite dissolution with the present-day coastline, coupled with limited recognition of dissolution-related collapse-brecciated carbonates in the Z2 carbonates offshore, might suggest that the dissolution occurred on uplift. The earlier the dissolution, the more widespread collapse brecciation would be in the subsurface: the absence of this evidence suggests it is uplift-related. A very recent episode of collapse is also possible: Pleistocene deposits with fossils (including elephant bones and seeds) are found within the collapse-brecciated Seaham Formation at Blackhall Rocks (Smith & Francis 1967 and references therein). The large volumes of fluids associated with deglaciation may well have promoted the dissolution of sulfate remaining in the shallow subsurface. The brecciation may have occurred in one or more discrete episodes. Further work is therefore needed to constrain the age(s) of dissolution, deformation and associated brecciation.

Significance for oil and gas exploration and production

Cross-border exploration may benefit from our work studying outcrop analogues in NE England because understanding the effects of evaporite dissolution will be useful in predicting fluid flow, reservoir quality and connectivity along the margins of palaeohighs which may have undergone historical exhumation and reburial (for example around the Utsira High, offshore Norway, that was exhumed in Jurassic times prior to reburial, Sorento *et al.* 2018). The findings hold relevance for any carbonates that have been subject to dissolution of an underlying unit and associated collapse, whether they be Z2, Z3 or of a completely different age.

The increased vertical and lateral connectivity within carbonates overlying completely dissolved evaporites could impact fluid flow both within a region and within an individual hydrocarbon accumulation. Strata that have undergone collapse due to evaporite dissolution may be of importance during later hydrocarbon migration, allowing hydrocarbons to breach zones where an impermeable layer originally existed. Evaporite dissolution around palaeohighs could have created leak points in regional seals, permitting migration of hydrocarbons from graben or basinal areas. The timing of dissolution relative to hydrocarbon migration is critical. If dissolution occurred early and was followed by (re-)burial with an overlying seal (for example following the Jurassic/Cretaceous erosion that affected the Auk Field, Trewin *et al.* 2003), charge can be retained and the collapse brecciated carbonate act as a reservoir. Awareness of potential leaks is also important for secure storage of carbon dioxide, should CO_2 be injected below an evaporite layer.

Recognition of this scenario on seismic data is indirect. The thinning of strata would be seismically resolvable (assuming 100–200 m of evaporite has been removed), although it is likely to be indistinguishable from other causes of thinned strata. The disturbance of the overlying strata can be imaged, however, as on the southern margin of the MNSH (Amiri-Garroussi & Taylor 1992, see also Taylor 1998 and references therein). Incorporating the structural history is necessary to further refine potential candidate breccias. Even with core diagnostic criteria, defining the cause of brecciation can be challenging to identify unequivocally; the key step in recognizing collapse breccias as such is to establish the presence of evaporites at a laterally equivalent stratigraphic level. A positive identification of a collapse breccia, however (as opposed to, for example, a mass-flow deposit), holds significance for the porosity and permeability in much of the overlying unit, not just the breccia body itself. Cores through Zone C might miss breccia bodies entirely, and so be hard to identify as collapsed strata, yet the whole sequence has enhanced flow properties.

Within an individual hydrocarbon accumulation, the collapsed carbonates will behave as a fractured reservoir (with production dominated by fracture permeability). The increase in matrix and fracture permeabilities associated with collapse will necessitate a modified production strategy as compared with an equivalent section that has not undergone collapse (for example, well spacing, production intervals and drainage rates). The lateral and vertical heterogeneity of the reservoir will be significant. The risk of losing significant volumes of mud while drilling will be elevated in the stratiform breccia and collapse-related faults, breccia pipes and fracture corridors. Significantly for the economics of a field the risk of early water breakthrough is increased as the lowest zone, Zone A, has greater permeability than the higher zones, so does not act as a barrier to the water leg. The relationship with the aquifer and flow rates within the aquifer needs to be well understood to ensure drawdown is not sufficiently high to encourage early water breakthrough. Focusing production from higher regions in Zone C would make use of the lower permeabilities up-section to reduce drawdown on the aquifer, potentially slowing water encroachment. Within the carbonate reservoir, the different deformation styles in limestone and dolomite (wide aperture fractures and greater incidence of breccia bodies respectively) could have implications for drainage rates of the different lithologies, and an increased risk of inefficient sweep/stranded hydrocarbons.

If evaporite dissolution were incomplete, layers of gypsum may remain as a horizontal barrier underneath the Z2 carbonate. It is likely that brecciation and fracturing would occur in the overlying carbonates; however, mobilized sulfate cements might seal many such fractures and occlude pores (‘anhydrite plugging’). This will greatly reduce the permeability. Thus, an uncertainty around a subsurface palaeohigh is whether the evaporite dissolution was complete, or whether incomplete dissolution could have reduced permeability.

Additionally, at some point basinward of a palaeohigh that has been subject to complete evaporite dissolution, there will be a gradual increase in residual anhydrite thickness offshore until attaining complete preservation of evaporite (Fig. 7). Using offshore NE England as an analogue this will be 4–8 km downdip of emergence (Fig. 7) and will represent a change in reservoir properties.

Fig. 20. Core photo taken from the collapse brecciated Argyll Field well 30/24-20 at *c.* 9801 m depth. The breccia has a clast-supported fabric with angular to subangular clasts, variable amounts of vuggy porosity and shows no sorting; the matrix comprises fine carbonate with variable amounts of clay. Photo based upon sample supplied under loan number: Core 225416 from well 30/24-20 BGS © UKRI.

Historical examples of collapsed carbonate reservoirs. Collapsed carbonates can be successful reservoirs, for example the Auk and Argyll fields in the UK CNS. The Zechstein carbonate reservoir in the Argyll Field, in UK block 30/24, is long-recognized as having undergone collapse brecciation (Gluyas *et al.* 2005), with collapse breccia visible in well core (Fig. 20). Commonly, cores taken in collapsed carbonates are highly fragmented with poor recovery. There have been three main episodes of production (Argyll was later renamed Ardmore and finally Alma, Gluyas *et al.* 2018) from four reservoirs (Jurassic sandstone, Rotliegend sandstone, Zechstein carbonate and Devonian sandstone and siltstone), with early production having focused almost entirely on the Zechstein carbonate. The Zechstein reservoir has a combined matrix and fracture porosity. There is pressure communication from the Zechstein carbonate through to the Devonian sandstone (good vertical communication). Strong aquifer support is provided through the high permeability Rotliegend sandstone. Six of the 16 wells produced from Zechstein carbonates exclusively (Table 2, see also Gluyas *et al.* 2018). The dissolution of evaporite in the Argyll Field was pre-Late Jurassic; the Jurassic interval over Argyll contains angular pebbles of Zechstein in a carbonate matrix with Jurassic fossils.

The Zechstein carbonate reservoir in the Auk Field, in UK Block 30/16, is also recognized as having been subject to collapse brecciation (Trewin *et al.* 2003). Production began in 1976, initially from Zechstein carbonates and later from Rotliegend sandstone. The Zechstein reservoir has dual porosity in vuggy fractured dolomite, similar to that of Argyll. Aquifer support was initially provided within the Zechstein dolomites then later from Rotliegend

Table 2. *Cumulative fluid production and yearly average total fluid production from Zechstein wells on the Argyll and Auk fields*

Field	Well	Production start	Production end	Years on production	Cumulative total fluid production (m^3)	Yearly average total fluid production (m^3)
Argyll	30/24- 02	01/06/1975	01/04/1979	3.84	1 739 502	409 358
Argyll	30/24- 05	01/07/1975	01/10/1992	17.27	2 724 190	157 963
Argyll	30/24- 06	01/06/1975	01/07/1982	7.09	1 119 366	160 673
Argyll	30/24- 08	01/12/1977	01/05/1978	0.41	36 531	89 100
Argyll	30/24- 12	01/02/1980	01/03/1982	2.08	3857	1659
Auk	A01S	01/02/1975	01/04/1986	7.66 (intermittent)	3 411 476	445 187
Auk	A04	01/12/1976	01/01/2000	23.1	12 580 476	544 642
Auk	A05	01/04/1977	01/01/2000	22.77	16 243 183	713 449
Auk	A07S	01/02/1985	01/01/2000	10.08 (intermittent)	677 694	67 199
Auk	A09	01/12/1979	01/08/1984	4.67	1 207 036	258 398
Auk	A12S1	01/01/1985	01/12/1995	3.58 (intermittent)	635 054	177 484
Auk	A13	01/05/1986	01/11/1989	3.51	960 312	273 839

Note that oil sourced in the Rotliegend and Devonian reservoirs also flowed into the Zechstein. Production data derived from BERR Well Production Data (2007).

sandstone. Six of the 22 wells produced from Zechstein carbonates exclusively (Table 2). Significantly, in both these two fields (Argyll and Auk) the facies and successions are interpreted to have been similar to that discussed in this paper (GRL 2016); they do not consist of shelf oolitic facies, the primary exploration target for Z2 carbonates.

Conclusions

Collapse breccias in the Zechstein Z2 carbonates of NE England were the result of dissolution of the underlying Hartlepool Anhydrite at shallow levels, on reaction with meteoric water. The timing of dissolution is not well constrained and could have occurred early after deposition, or during the Triassic or during late Cretaceous– early Tertiary uplift; it is possible that more than one event occurred at different times. The Roker Formation collapsed into the underlying spaces, causing fundamental changes in stratal architecture. Three zones within the collapsed rock are identified, the development of which is influenced by the mechanical layering through the collapsed section, with decreasing deformation intensity up-section. At the base, the lowermost zone (A) is composed of a massive stratiform breccia immediately above the dissolved anhydrite, with increased fracture and matrix permeability. The overlying zone (B) is predominantly a crackle breccia, with discrete breccia bodies. The upper layer (C) which is the thickest and extends to the top of the Roker Formation, maintains primary fabrics (i.e. bedding), has broad-scale open folding, localized breccia and faulting. Within the uppermost two zones breccia pipes develop with significant vertical permeability, in addition to collapse-related faults and fracture corridors, all of which could act as fluid conduits in the subsurface. The degree of brecciation of carbonates overlying a dissolved evaporite depends on the nature of the original lithologies and their competences. We suggest that the variation in mechanical properties vertically within a collapsing succession will control the distribution and intensity of deformation up-section.

Collapsed carbonates can make good reservoirs, as evidenced by Argyll and Auk fields in the UK Central North Sea, but the collapse has implications for hydrocarbon extraction in terms of field development planning (well trajectories, production intervals and drainage rates) as compared with equivalent 'un-collapsed' carbonates. The sequence of events associated with collapse is likely to be a gradual process, with local variations in the extent of collapse, with enhanced dissolution along faults and fractures within the anhydrite and correspondingly enhanced collapse above.

Acknowledgements The authors thank Geospatial Research Ltd for allowing publication of this material. We thank Stefano Patruno, Ross Grant, Ann Watkins, Joel Corcoran and Arild Eliassen for their thorough reviews. MET is grateful to Adrian Immenhauser (Ruhr Universitat) for kindly providing isotope analyses and to Joao Paulo Gomes for adjusting some figures. David Oxlade and Sebastien Gilment of GRL are both thanked for their help generating ortho-rectified images of the cliff section.

Funding This work was undertaken in 2015–16 as part of a proprietary study by Geospatial Research Ltd (GRL) on the fracture properties, stratigraphy, diagenesis and production history of Zechstein carbonates.

Author contributions **SED**: conceptualization (equal), investigation (equal), project administration (lead), visualization (lead), writing – original draft (lead), writing – review & editing (equal); **MET**: conceptualization (equal), data curation (equal), formal analysis (lead), investigation (equal), supervision (equal), writing – original draft (supporting), writing – review & editing (lead); **MJM**: conceptualization (equal), investigation (equal), supervision (equal), writing – review & editing (supporting); **REH**: conceptualization (supporting), investigation (supporting), validation (supporting), writing – review & editing (supporting); **JJL**: data curation (supporting), investigation (supporting); **JGG**: validation (supporting), writing – review & editing (supporting); **RRJ**: writing – review & editing (supporting).

References

Amiri-Garroussi, K. & Taylor, J.C.M. 1992. Displaced carbonates in the Zechstein of the UK North Sea. *Marine and Petroleum Geology*, **9**, 186–196, https://doi.org/10.1016/0264-8172(92)90090-2

Aplin, G.F. 1981. *Diagenesis of the Zechstein Main Reef Complex, N.E. England*. Institute of Geological Sciences Stable Isotope Report, **66**.

BERR 2007. Well Production Data https://itportal.ogauthority.co.uk/information/wells/pprs/Well_production_offshore_oil_fields/offshore_oil_fields_by_well/offshore_oil_fields_by_well.htm [last accessed September 2015]

Cantrell, D.L., Al-Khammash, A. & Jenden, P.D. 2007. Characterization and significance of dedolomite in Wadi Nisah, central Saudi Arabia. *GeoArabia*, **12**, 15–30.

Catuneanu, O., Galloway, W.E., Kendall, C.G.S.C., Miall, A.D., Posamentier, H.W., Strasser, A. & Tucker, M.E. 2011. Sequence stratigraphy: methodology and nomenclature. *Newsletters on Stratigraphy*, **44**, 173–245, https://doi.org/10.1127/0078-0421/2011/0011

Clark, D.N. 1980. The diagenesis of Zechstein carbonate sediments. *In*: Füchtbauer, H. & Peryt, T. (eds) *The Zechstein Basin with Emphasis on Carbonate Sequences*. Contributions to Sedimentology, **9**, 167–203.

Cooke, M.L., Simo, J.A., Underwood, C.A. & Rijken, P. 2006. Mechanical stratigraphic controls on fracture patterns within carbonates and implications for groundwater flow. *Sedimentary Geology*, **184**, 225–239, https://doi.org/10.1016/j.sedgeo.2005.11.004

Cooper, A.H. 1986. Subsidence and foundering of strata caused by the dissolution of Permian gypsum in the Ripon and Bedale areas, North Yorkshire. *In*: Harwood, G.M. & Smith, D.B. (eds) *The English Zechstein and Related Topics*. Geological Society, London, Special Publications, **22**, 127–139, https://doi.org/10.1144/GSL.SP.1986.022.01.11

Doornenbal, H. & Stevenson, A. 2010. *Petroleum Geological Atlas of the Southern Permian Basin Area*. EAGE, Houten.

Eliassen, A. & Talbot, M.R. 2005. Solution-collapse breccias of the Minkinfjellet and Wordiekammen Formations, Central Spitsbergen, Svalbard: a large gypsum palaeokarst system. *Sedimentology*, **52**, 775–794, https://doi.org/10.1111/j.1365-3091.2005.00731.x

Elvebakk, G., Hogstad, K., Hunt, D., Pajchel, K., Rafaelsen, B. & Robak, H. 2003. Upper Carboniferous–Lower Permian Gipsdalen Group karstified reservoir carbonates of the Loppa High, Barents Sea; reservoir potential and drilling challenges. *Proceedings Conference on Petroleum Exploration and Production in Environmentally Sensitive Areas*, Ålesund.

Evans, A.L., Fitch, F.J. & Miller, J.A. 1973. Potassium–argon age determinations on some British Tertiary Igneous rocks. *Journal of the Geological Society, London*, **129**, 419–443, https://doi.org/10.1144/gsjgs.129.4.0419

Ford, D.C. & Williams, P.W. 1989. *Karst Geomorphology and Hydrology*. Unwin Hyman, London.

Fossen, H. 2016. *Structural Geology*. Cambridge University Press, Cambridge.

Frenzel, M. & Woodcock, N.H. 2014. Cockade breccia: Product of mineralisation along dilational faults. *Journal of Structural Geology*, **68**, 194–206, https://doi.org/10.1016/j.jsg.2014.09.001

Friedman, G.M. 1997. Dissolution-collapse breccias and palaeokarst resulting from dissolution of evaporite rocks, especially sulfates. *Carbonates and Evaporites*, **12**, 53–63.

Fyfe, J.A., Gregersen, U. *et al.* 2003. Oligocene to Holocene *In*: Evans, D., Graham, C., Armour, A. & Bathurst, P. (eds) *The Millennium Atlas: Petroleum Geology of the Central and Northern North Sea*. Geological Society, London, Special Publications, **279**, 279–287.

Geluk, M. 1999. Late Permian (Zechstein) rifting in the Netherlands; models and implications for petroleum geology. *Petroleum Geoscience*, **5**, 189–199, https://doi.org/10.1144/petgeo.5.2.189

Genna, A., Jébrak, M., Marcoux, E. & Milési, J.P. 1996. Genesis of cockade breccias in the tectonic evolution of the Cirotan epithermal gold system, West Java. *Canadian Journal of Earth Sciences*, **33**, 93–102, https://doi.org/10.1139/e96-010

Gluyas, J.G., Mair, B., Schofield, P., Arkley, P. & McRae, D. 2005. Ardmore Field: rebirth of the first offshore oil field, UKCS. *In*: Doré, A.G. & Vining, B.A. (eds) *Petroleum Geology: North-West Europe and Global Perspective*. Geological Society, London, Petroleum Geology Conference Series, **6**, 367–388, https://doi.org/10.1144/0060367

Gluyas, J., Tang, L. & Jones, S. 2018. Argyll Field: the first oil field to be developed on the UK Continental Shelf. *In*: Craig, J., Gerali, F., MacAulay, F. & Sorkhabi, R. (eds) *History of the European Oil and Gas Industry*. Geological Society, London, Special Publications, **465**, 77–93, https://doi.org/10.1144/SP465.3

Grant, R.J., Underhill, J.R., Hernández-Casado, J., Barker, S.M. & Jamieson, R.J. 2019. Upper Permian Zechstein Supergroup carbonate–evaporite platform palaeomorphology in the UK Southern North Sea. *Marine and Petroleum Geology*, **100**, 484–518, https://doi.org/10.1016/j.marpetgeo.2017.11.029

Green, P.F. 1986. On the thermo-tectonic evolution of Northern England: evidence from fission track analysis. *Geological Magazine*, **123**, 493–506, https://doi.org/10.1017/S0016756800035081

Green, P.F., Duddy, I.R. & Japsen, P. 2018. Multiple episodes of regional exhumation and inversion identified in the UK Southern North Sea based on integration of palaeothermal and palaeoburial indicators. *In*: Bowman, M. & Levell, B. (eds) *Petroleum Geology of NW Europe: 50 Years of Learning*. Geological Society, London, Petroleum Geology Conference Series, **8**, 47–65, https://doi.org/10.1144/PGC8.21

GRL (Geospatial Research Ltd) 2016. Proprietary study on the stratigraphy, diagenesis, fracture properties and production history of Zechstein carbonates.

Gutiérrez, F., Guerrero, J. & Lucha, P. 2008. A genetic classification of sinkholes illustrated from evaporite palaeokarst exposures in Spain. *Environmental Geology*, **53**, 993–1006, https://doi.org/10.1007/s00254-007-0727-5

Harwood, G.M. 1986. The diagenetic history of the Cadeby Formation (EZ1 Ca), Upper Permian, eastern England. *In*: Harwood, G.M. & Smith, D.B. (eds) *The English Zechstein and Related Topics*. Geological Society, London, Special Publications, **22**, 75–86, https://doi.org/10.1144/GSL.SP.1986.022.01.07

Hauck, T.E., Corlett, H.J., Grobe, M., Walton, E.L. & Jofre, P.S. 2018. Meteoric diagenesis and dedolomite fabrics in precursor primary dolomicrite in a mixed carbonate–evaporite system. *Sedimentology*, **65**, 1827–1858, https://doi.org/10.1111/sed.12448

Hillis, R.R., Holford, S.P. *et al.* 2008. Cenozoic exhumation of the southern British Isles. *Geology*, **36**, 371–374, https://doi.org/10.1130/G24699A.1

James, A.H., Cooper, A.H. & Holliday, D.W. 1981. Solution of the gypsum cliff (Permian, Middle Marl), by the River Ure at Ripon Parks, North Yorkshire. *Proceedings of the Yorkshire Geological Society*, **43**, 433–450, https://doi.org/10.1144/pygs.43.4.433

Jiang, L., Worden, R.H., Cai, C.F., Shen, A. & Crowley, S.F. 2018. Diagenesis of an evaporite related carbonate reservoir in deeply buried Cambrian strata, Tarim Basin, northwest China. *AAPG Bulletin*, **102**, 77–102, https://doi.org/10.1306/0328171608517048

Jowett, E.C., Cathles, L.M. & Davis, B.W. 1993. Predicting the dehydration of gypsum in evaporitic sedimentary basins. *AAPG Bulletin*, **77**, 402–413.

Kimbell, G.S.K., Young, B., Millward, D. & Crowley, Q.G. 2010. The North Pennine batholith (Weardale Granite) of northern England: new data on its age and form. *Proceedings of the Yorkshire Geological Society*, **58**, 107–128, https://doi.org/10.1144/pygs.58.1.273

Kirkham, A. 2011. Halite, sulphates, sabkhas and salinas of the coastal regions and Sabkha Matti of Abu Dhabi, United Arab Emirates. *In*: Kendall, C.G.St.C. & Alsharhan, A.S. (eds) *Quaternary Carbonate and Evaporite Sedimentary Facies and their Ancient Analogues*. International Association of Sedimentologists Special Publication, **43**, 265–276.

Kirkham, A. & Evans, G. 2019. Aspects of the Abu Dhabi Sabkha. *In*: Gul, B., Böer, B., Khan, M., Clüsener-Godt, M. & Hameed, A. (eds) *Sabkha Ecosystems. Tasks for Vegetation Science*, **49**. Springer.

Klimchouk, A. & Aksem, S.D. 2005. Hydrochemistry and solution rates in gypsum karst: case study from the Western Ukraine. *Environmental Geology*, **48**, 307–319, https://doi.org/10.1007/s00254-005-1277-3

Klimchouk, A., Cucchi, F, Calaforra, J.M., Aksem, S.D., Finocchiaro, F. & Forti, P. 1996. Dissolution of gypsum from field observations. *International Journal of Speleology*, **25**, 37–48, https://doi.org/10.5038/1827-806X.25.3.3

Lebour, G.A. 1884. On the breccia-gashes of the Durham coast and some recent earth-shakes at Sunderland. *Transactions of the North of England Institute of Mining and Mechanical Engineers*, **33**, 165–177, https://doi.org/10.1017/S0016756800132121

Lee, M.R. 1993. Formation and diagenesis of slope limestones within the Upper Permian (Zechstein) Raisby Formation, north-east England. *Proceedings of the Yorkshire Geological Society*, **49**, 215–227, https://doi.org/10.1144/pygs.49.3.215

Lee, M.R. 1994. Emplacement and diagenesis of gypsum and anhydrite in the late Permian Raisby Formation, north-east England. *Proceedings of the Yorkshire Geological Society*, **50**, 143–155, https://doi.org/10.1144/pygs.50.2.143

Lee, M.R. & Harwood, G.M. 1989. Dolomite calcitization and cement zonation related to exhumation of the Raisby Formation (Zechstein carbonate), northeast England. *Sedimentary Geology*, **65**, 285–305, https://doi.org/10.1016/0037-0738(89)90030-4

Liu, L., Ding, X., Cao, J., Yang, G. & Ma, T. 2019. Eogenetic karst in interbedded carbonates and evaporites and its impact on hydrocarbon reservoirs: a new case from the Middle Triassic Leikoupo Formation in Sichuan Basin, Southwest China. *Journal of Earth Sciences*, **30**, 908–923, https://doi.org/10.1007/s12583-019-0888-7

Loucks, R.G. 1999. Palaeocave carbonate reservoirs: origins, burial-depth modifications, spatial complexity, and reservoir implications. *AAPG Bulletin*, **83**, 1795–1834, https://doi.org/10.1306/E4FD426F-1732-11D7-8645000102C1865D

Lovell, J.P.B. 1984. Cenozoic. *In*: Glennie, K.W. (ed.) *Introduction to the Petroleum Geology of the North Sea*. Blackwell, London, 151–169.

Mawson, M. & Tucker, M.E. 2009. High-frequency cyclicity (Milankovitch and millennial-scale) in slope-apron carbonates: Zechstein (Upper Permian), North-east England. *Sedimentology*, **56**, 1905–1936, https://doi.org/10.1111/j.1365-3091.2009.01062.x

Menezes, D.F., Bezerra, F.H., Balsamo, F., Arcari, A., Maia, R.P. & Cazarin, C.L. 2019. Subsidence rings and fracture pattern around dolines in carbonate platforms: Implications for evolution and petrophysical properties of collapse structures. *Marine and Petroleum Geology*, **113**, 104113, https://doi.org/10.1016/j.marpetgeo.2019.104113

Monaghan, A.A., Arsenikos, S. *et al.* 2017. Carboniferous petroleum systems around the Mid North Sea High, UK. *Marine and Petroleum Geology*, **88**, 282–302, https://doi.org/10.1016/j.marpetgeo.2017.08.019

Musset, A.E., Dagley, P. & Skelhorn, R.R. 1988. Time and duration of activity in the British Tertiary Igneous

Province. *In*: Morton, A.C. & Parson, L.M. (eds) *Early Tertiary Volcanism and the Opening of the North Atlantic*. Geological Society, London, Special Publications, **39**, 337–348, https://doi.org/10.1144/GSL.SP.1988.039.01.29

Patruno, S. & Helland-Hansen, W. 2018. Clinoform systems: review and dynamic classification scheme for shorelines, subaqueous deltas, shelf edges and continental margins. *Earth-Science Reviews*, **185**, 202–233, https://doi.org/10.1016/j.earscirev.2018.05.016

Patruno, S., Reid, W., Jackson, C.A-L. & Davies, C., 2018. New insights into the unexploited reservoir potential of the Mid North Sea High (UKCS Quadrants 35-38, 41-43): a newly-described intra Zechstein sulphate-carbonate platform complex. *In*: Bowman, M. & Levell, B. (eds) *Petroleum Geology of NW Europe: 50 Years of Learning*. Geological Society, London, Petroleum Geology Conference Series, **8**, 87–124, https://doi.org/10.1144/PGC8.9

Patruno, S., Reid, W., Berndt, C. & Feuilleaubois, L. 2019. Polyphase tectonic inversion and its role in controlling hydrocarbon prospectivity in the Greater East Shetland Platform and Mid North Sea High, offshore UK. *In*: Monaghan, A.A., Underhill, J.R., Hewett, A.J. & Marshall, J.E.A. (eds) *Palaeozoic Plays of NW Europe*. Geological Society, London, Special Publications, **471**, 177–235, https://doi.org/10.1144/SP471.9

Paul, J. 2014. Gypsum domes and diapirs: common features in the Zechstein (Upper Permian) of Germany. *Geological Quarterly*, **58**, 521–530, https://doi.org/10.7306/gq.v58i3.13646

Perri, E., Tucker, M.E. & Mawson, M. 2013. Biotic and abiotic processes in the formation and diagenesis of Permian dolomitic stromatolites (Zechstein, NE England). *Journal of Sedimentary Research*, **83**, 896–914, https://doi.org/10.2110/jsr.2013.65

Pettigrew, T.H. 1980. Geology. *In*: Dunn, T.C. (ed.) *The Magnesian Limestone of Durham County*. Durham County Conservation Trust, Durham, UK, 4–26.

Richardson, N.J., Allen, M.R. & Underhill, J.R. 2005. Role of Cenozoic fault reactivation in controlling pre-rift plays, and the recognition of Zechstein Group evaporite-carbonate lateral facies transitions in the East Orkney and Dutch Bank basins, East Shetland Platform, UK North Sea. *In*: Doré, A.G. & Vining, B.A. (eds) *Petroleum Geology: North-West Europe and Global Perspective*. Geological Society, London, Petroleum Geology Conference Series, **6**, 337–348, https://doi.org/10.1144/0060337

Richter-Bernburg, G. 1985. Zechstein-Anhydrite: facies und genese. *Geologisches Jahrbuch (Reihe A)*, **85**, 3–85.

Robson, D. 1991. The Argyll, Duncan and Innes Fields, Block 30/24 and 30/25a, UK North Sea. *In*: Abbotts, I.L. (ed.) *United Kingdom Oil and Gas Fields, 25 Years Commemorative Volume*. Geological Society, London, Memoirs, **14**, 219–226, https://doi.org/10.1144/GSL.MEM.1991.014.01.27

Sando, W.J. 1967. Madison Limestone (Mississippian), Wind River, Washakie, and Owl Creek Mountains, Wyoming. *AAPG Bulletin*, **51**, 529–557.

Schoenherr, J., Reuning, L. *et al.* 2018. Dedolomitization: review and case study of uncommon mesogenetic formation conditions. *Earth-Science Reviews*, **185**, 780– 805, https://doi.org/10.1016/j.earscirev.2018.07.005

Sedgwick, A. 1829. On the geological relations and internal structure of the Magnesian Limestone, and the lower portions of the New Red Sandstone in their range through Nottinghamshire, Derbyshire, Yorkshire and Durham, to the southern extremity of Northumberland. *Transactions of the Geological Society of London*, **3**, 37–124, https://doi.org/10.1144/transgslb.3.1.37

Słowakiewicz, M., Tucker, M.E., Perri, E. & Pancost, R.D. 2015*a*. Nearshore euxinia in the photic zone of an ancient sea. *Palaeogeography, Palaeoclimatology, Palaeoecology*, **426**, 242–259, https://doi.org/10.1016/j.palaeo.2015.03.022

Słowakiewicz, M., Tucker, M.E., Vane, C.H., Harding, R., Collins, A. & Pancost, R.D. 2015*b*. Shale-gas potential of the Mid-Carboniferous Bowland-Hodder Unit, Cleveland Basin (Yorkshire) Central Britain. *Journal of Petroleum Geology*, **38**, 59–76, https://doi.org/10.1111/jpg.12598

Smith, D.B. 1970. Submarine slumping and sliding in the Lower Magnesian Limestone of Northumberland and Durham. *Proceedings of the Yorkshire Geological Society*, **38**, 1–36, https://doi.org/10.1144/pygs.38.1.1

Smith, D.B. 1972. Foundered strata, collapse-breccias and subsidence features of the English Zechstein. *In*: Richter-Bernburg, G. (ed.) *Geology of Saline Deposits*. Earth Sciences **7**, UNESCO, 255–269.

Smith, D.B. 1980. The evolution of the English Zechstein Basin. *In*: Füchtbaeur, H. & Peryt, T.M. (eds) *The Zechstein Basin with Emphasis on Carbonate Sequences*. Contributions to Sedimentology, Elsevier, Amsterdam, **9**, 7–34.

Smith, D.B. 1986. The Trow Point Bed – a deposit of Upper Permian marine oncoids, peloids and stromatolites in the Zechstein of NE England. *In*: Harwood, G.M. & Smith, D.B. (eds) *The English Zechstein and Related Topics*. Geological Society, London, Special Publications, **22**, 113–125, https://doi.org/10.1144/GSL.SP.1986.022.01.10

Smith, D.B. 1989. The late Permian palaeogeography of northeast England. *Proceedings of the Yorkshire Geological Society*, **47**, 285–312, https://doi.org/10.1144/pygs.47.4.285

Smith, D.B. 1994. *Geology of the country around Sunderland.* Memoir of the British geological Survey. Sheet 21 (England and Wales). British Geological Survey, Nottingham.

Smith, D.B. 1995. *Marine Permian of England*. Geological Conservation Review Series, **8**, Chapman and Hall, London.

Smith, D.B. & Francis, E.A. 1967. *Geology of the country between Durham and West Hartlepool*. Memoir of the Geological Survey of Great Britain, Sheet 27 (England and Wales). HMSO.

Smith, D.B., Harwood, G.M., Pattison, J. & Pettigrew, T.H. 1986. A revised nomenclature for Upper Permian strata in eastern England. *In*: Harwood, G.M. & Smith, D.B. (eds) *The English Zechstein and Related Topics*. Geological Society, London, Special Publications, **22**, 9–17, https://doi.org/10.1144/GSL.SP.1986.022.01.02

Sorento, T., Stemmerik, L. & Olaussen, S. 2018. Upper Permian carbonates at the northern edge of the Zechstein basin, Utsira High, Norwegian North Sea. *Marine and Petroleum Geology*, **89**, 635–652, https://doi.org/10.1016/j.marpetgeo.2017.10.030

Stanton, R.J. 1966. The solution brecciation process. *Bulletin of the Geological Society of America*, **77**, 843–848.

Strohmenger, C., Voigt, E. & Zimdars, J. 1996. Sequence stratigraphy and cyclic development of Basal Zechstein carbonate-evaporite deposits with emphasis on Zechstein 2 off-platform carbonates (Upper Permian, Northeast Germany). *Sedimentary Geology*, **102**, 33–54, https://doi.org/10.1016/0037-0738(95)00058-5

Taylor, J.C.M. 1998. Upper Permian–Zechstein. *In*: Glennie, K.W. (ed.) *Petroleum Geology of the North Sea: Basic Concepts and Advances*. 4th ed. Blackwell, 174–211.

Trechmann, C.T. 1914. On the lithology and composition of Durham Magnesian Limestones. *Quarterly Journal of the Geological Society of London*, **70**, 232–265, https://doi.org/10.1017/S0016756800201854

Trewin, N.H. & Bramwell, G.M. 1991. The Auk Field, Block 30/16, UK North Sea. *In*: Abbotts, I.L. (ed.) *United Kingdom Oil and Gas Fields, 25 Years Commemorative Volume*. Geological Society, London, Memoirs, **14**, 227–236, https://doi.org/10.1144/GSL.MEM.1991.014.01.28

Trewin, N.H., Fryberger, S.G. & Kreutz, H. 2003. The Auk Field, Block 30/16, UK North Sea. *In*: Gluyas, J.G. & Hichens, H.M. (eds) *United Kingdom Oil and Gas Fields: Commemorative Millennium volume*. Geological Society, London, Memoirs, **20**, 485–496, https://doi.org/10.1144/GSL.MEM.1991.014.01.28

Tucker, M.E. 1991. Sequence stratigraphy of carbonate-evaporite basins: models and application to the Upper Permian (Zechstein) of northeast England and adjoining North Sea. *Journal of the Geological Society, London*, **148**, 1019–1036, https://doi.org/10.1144/gsjgs.148.6.1019

Tucker, M.E. & Hollingworth, N.T.J. 1986. The upper Permian reef complex (EZ1) of North East England. *In*: Schroeder, J.H. & Purser, B.H. (eds) *Reef Diagenesis*. Springer-Verlag, Berlin, 270–290.

Vincent, C J. 2015. *Maturity Modelling of Selected Wells in the Central North Sea*. British Geological Survey Internal Report, **CR/15/122**.

Warren, J.K. 2006. *Evaporites: Sediments, Resources and Hydrocarbons*. Springer Science and Business Media.

Winch, N.J. 1817. I. Observations on the Geology of Northumberland and Durham. *Transactions of the Geological Society of London*, **1**, 1–101, https://doi.org/10.1144/transgsla.4.1

Woolacott, D. 1909. A case of thrust and crush-brecciation in the Magnesian Limestone, County Durham. *The University of Durham Philosophical Society Memoir*, **1**, 16, https://doi.org/10.1016/S0016-7878(13)80005-3

Woolacott, D. 1912. The stratigraphy and tectonics of the Permian of Durham (northern area) and Northumberland. *Proceedings of the University of Durham Philosophical Society*, **4**, 241–331.

Zeigler, P.A. 1981. Evolution of sedimentary basins in north-west Europe. *In*: Illing, L.V. & Hobson, G.D. (eds) *Petroleum Geology of the Continental Shelf of Northwest Europe*. Heyden, London, 3–39.